Next generation lipopeptide antibiotics

Al Ayed, U.K.

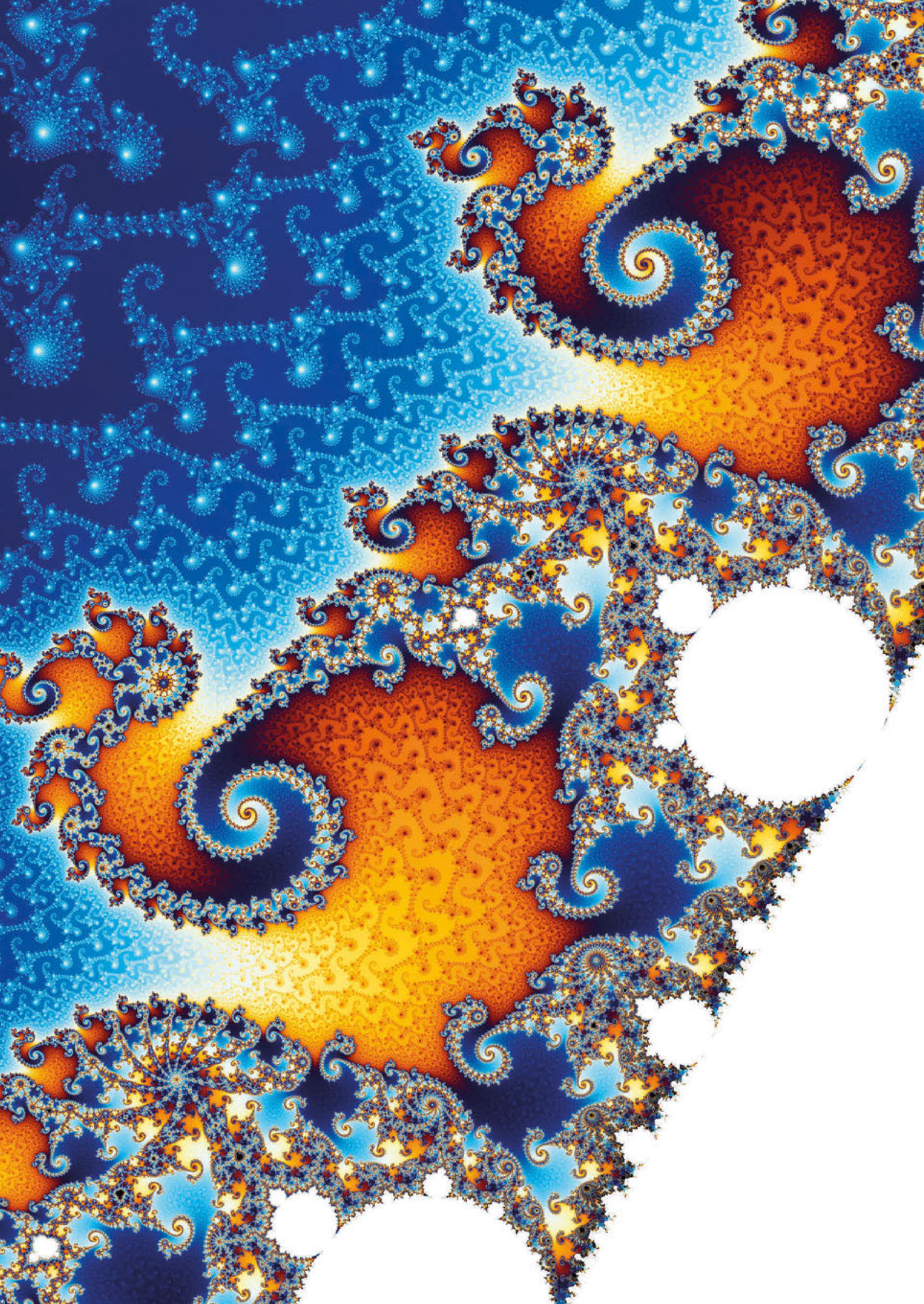

Chapter 5

Total Synthesis and Structure Assignment of the Relacidine Lipopeptide Antibiotics and Preparation of Analogues with Enhanced Stability

Abstract

The unabated rise of antibiotic resistance has raised the specter of a post-antibiotic era underscoring the importance of developing new classes of antibiotics. The relacidines are a recently discovered group of non-ribosomal lipopeptide antibiotics that show promising activity against Gram-negative pathogens and share structural similarities with brevicidine and laterocidine. While the first reports of the relacidines indicated that they possess a C-terminal five-amino acid macrolactone, an N-terminal lipid tail, and an overall positive charge, no stereochemical configuration was assigned precluding a full structure determination. To address this issue we here report a bioinformatics guided total synthesis of relacidine A and B and show that the authentic natural products match our predicted and synthesized structures. Following on this, we also synthesized an analogue of relacidine A wherein the ester linkage of the macrolactone was replaced by the corresponding amide. This analogue was found to possess enhanced hydrolytic stability while maintaining the antibacterial activity of the natural product in both *in vitro* and *in vivo* efficacy studies.

Parts of this chapter have been published in ACS Infectious Diseases:

Al Ayed, K.; Zamarbide Losada, D.; Machushynets, N. V.; Terlouw, B.; Elsayed, S. S.; Schill, J.; Trebosc, V.; Pieren, M.; Medema, M. H.; van Wezel, G. P.; Martin, N. I. Total Synthesis and Structure Assignment of the Relacidine Lipopeptide Antibiotics and Preparation of Analogues with Enhanced Stability. *ACS Infect Dis* **2023**, *9* (4), 739–748. https://doi.org/10.1021/acsinfecdis.3c00043.

Parts of the data in this chapter are part of a patent:

"Antibiotic natural product analogues"; Cochrane, S.A.; Ballantine, R. D.; Martin, N. I.; Al Ayed, K.; Hoekstra, M.; Zamarbide Losada, S.D.; Priority Date: 28 January 2021; Published: 4 August 2022; WO2022162332A1

Introduction

Antimicrobial resistance (AMR) is recognized as a serious threat to public health today and has been projected to become a major global health crisis in the near future. A recently published study estimated that in 2019 there were 4.95 million deaths associated with bacterial AMR, including 1.27 million deaths directly attributable to AMR.[1] Beyond these current numbers, some have estimated that AMR could kill upwards of 10 million people per year globally by 2050.[2,3] Moreover, a recent report from the US Centers for Disease Control and Prevention found that the COVID-19 pandemic has further accelerated the spread of AMR, particularly in hospital settings.[4] In assessing the threat posed by AMR, the so-called ESKAPE pathogens have risen to prominence comprising: *Enterococcus faecium*, *Staphylococcus aureus*, *Klebsiella pneumoniae*, *Acinetobacter baumannii*, *Pseudomonas aeruginosa*, and *Enterobacter* species.[5] These pathogens are prone to developing antibiotic resistance and the infections they cause are often difficult to treat. Notable among the ESKAPE pathogens are the Gram-negative species which the World Health Organization has exclusively categorized as threat-level 'critical'. While there is a dire need for antibacterial agents that can effectively combat these particularly dangerous Gram-negative bacteria, the development of new antibiotics has stagnated since the 1980s.[6] Clearly, innovative approaches are needed to discover and develop new antibiotics that act against these pathogens.

In 2018, Qian and coworkers reported two new lipopeptide antibiotics discovered by mining bacterial genomes.[7] These natural products, termed brevicidine and laterocidine (Fig. 1), were found to exhibit potent anti-Gram-negative specific activity and low eukaryotic cell toxicity.

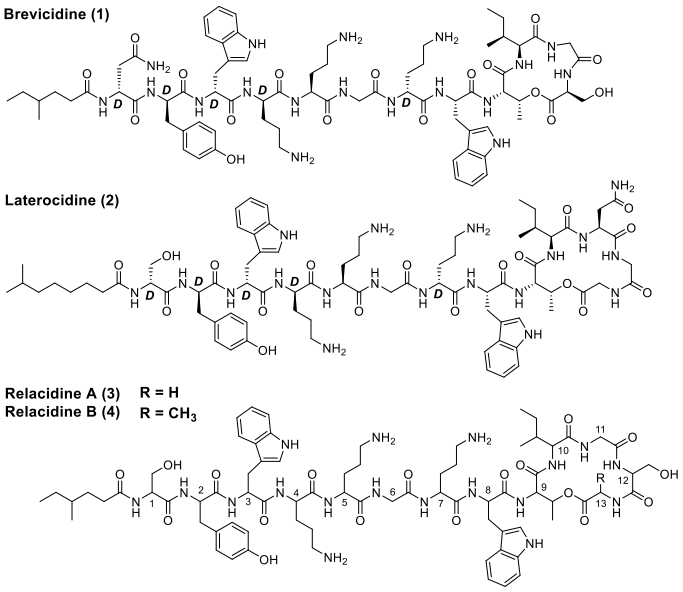

Figure 1. Structures of brevicidine (**1**), laterocidine (**2**), and previously proposed structures for relacidine A (**3**) and B (**4**). For the structures of brevicidine and laterocidine D-amino acids labeled D. Amino acid numbering indicated for relacidine A and B.

The low yields associated with the isolation of brevicidine and laterocidine via fermentative methods prompted us to pursue a total synthesis approach for their production which we also recently reported.[8] Shortly after brevicidine and laterocidine were discovered, the Kuipers group reported a series of structurally similar lipopeptides they named the relacidines.[9] As for brevicidine and laterocidine, the relacidines were found to specifically affect the growth of Gram-negative bacteria via a mechanism involving interactions with lipopolysaccharide (LPS).[9] Based on the relacidine biosynthetic gene clusters, and subsequent NMR and mass-spectrometric analysis of the natural products isolated, the Kuipers group proposed two main relacidine structures: relacidine A and relacidine B (Fig. 1).

While the stereochemical configurations of the amino acids comprising relacidine A and B were not assigned in the original report, the compounds are clearly similar in structure to brevicidine and laterocidine. In terms of their primary sequences, relacidine A and B differ only in the C-terminal residue that is esterified with the side chain of Thr9 to form the macrolactone. In relacidine A this C-terminal residue is Gly, while in relacidine B it is Ala (Fig. 1). In comparing the relacidines to brevicidine and laterocidine, it is apparent that they more closely resemble laterocidine. The sequence of the exocyclic linear peptide is the same for the relacidines and laterocidine and they also both have a five-amino acid macrocycle, while the brevicidine macrocycle consists of four residues. It is in the amino acids of the macrocycle that the relacidines differ from laterocidine. Specifically, the three C-terminal residues in the relacidines are Gly11, Ser12, and Gly13/Ala13 while in laterocidine they are Asn11, Gly12, and Gly13. These differences, and the lack of stereochemical assignments, prompted us to consider a total synthesis approach to the relacidines as a means of unambiguously establishing their structures. Furthermore, as for brevicidine and laterocidine, isolation of the relacidines from fermentation of the producing organism *Brevibacillus laterosporus*, requires laborious purification while yielding low quantities of pure material (sub-milligram per liter). In such cases total synthesis can provide an attractive alternative for obtaining quantities of material suitable for more comprehensive studies. To this end, we here report the total synthesis of a series of relacidine A and B diastereomers that, when compared with the natural product, allowed for unambiguous stereochemical assignments. In addition, we describe the synthesis of an analogue of relacidine A that exhibits increased stability in serum while retaining potent *in vitro* activity against a number of Gram-negative pathogens and *in vivo* activity in an established *Galleria mellonella* larvae infection model.

Results and Discussion

Prior to embarking on the synthesis of relacidine A and B, we used a bioinformatics-based approach to predict the stereochemical configuration of the amino acids. To this end, we first analyzed the genome of *Brevibacillus laterosporus* MG64 (GenBank accession NZ_QJJD01000001), the producing strain originally characterized by Kuipers and coworkers, using antiSMASH (v6.0.0; default settings).[9,10,11] This allowed us to readily identify the relacidine biosynthetic gene cluster (BGC, see Supplemental Information) based on biosynthetic logic. Subsequently, the architecture of the non-ribosomal peptide synthetase (NRPS) modules that assemble the relacidine peptide scaffold were studied. Particularly, we determined which modules contain epimerization domains, i.e. domains which catalyze the conversion from an L- to D-amino acid. Modules 1, 2, 3, 4, and 7 of *rlcC*, which incorporate serine, tyrosine,

tryptophan, ornithine, and ornithine, respectively, were all predicted to contain epimerization domains (Fig. 2A). Therefore, these residues were predicted to have a D-configuration in the final relacidine scaffold. To further confirm this, the relacidine BGC was compared to those of brevicidine and laterocidine, using the MIBiG database (MIBiG accessions BGC0001536 and BGC0002432 respectively), which showed that, barring a missing terminal module in the brevicidine BGC, the module architectures of all three BGCs are identical.[12] As the stereochemical configurations of brevicidine and laterocidine have been fully assigned, we could confirm that the epimerization domains in the brevicidine and laterocidine BGCs correspond exactly to the positions of the D-amino acids observed in their respective products.[7] Therefore, we predicted that the relacidines likely have the same stereochemical configurations at the same amino acid positions compared to brevicidine and laterocidine (Fig. 2B).

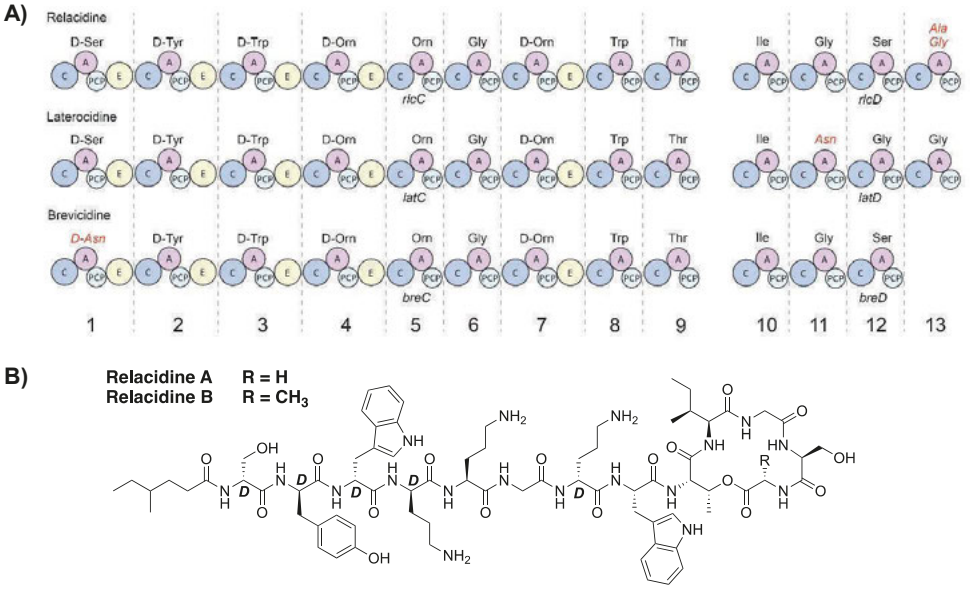

Figure 2. Comparison of the relacidine, laterocidine, and brevicidine biosynthetic gene clusters. A) Architecture of the NRPS modules of the relacidine, laterocidine, and brevicidine BGCs. **B)** Predicted chemical structures of relacidine A and B including stereochemical assignments. (C=Condensation domain; A=Adenylation domain; PCP=Peptidyl Carrier Protein domain; E=Epimerization domain). D-amino acids labeled D.

The peptide backbones of the relacidines, brevicidine, and laterocidine show differences at various positions (Fig. 2A). We analyzed the genetic basis for these differences by examining the active site sequences of the adenylation (A) domains, which are responsible for selecting the amino acid building blocks in non-ribosomal peptide biosynthesis. We uncovered a curious difference between the relacidine and laterocidine BGCs in the fourth module of *rlcD* (*latD*), which incorporates Gly in laterocidine biosynthesis and either Ala or Gly in relacidine biosynthesis.

Specifically, the relacidine BGC encodes Tyr at position 290, while the laterocidine BGC encodes Trp at the same position (labeled as position 291 in the laterocidine BGC). This difference is notable as this residue is centrally located in the active site of the A-domain that incorporates the 13th amino acid of relacidine and laterocidine (Fig. 3A). Given that the only difference between relacidine A and B is the incorporation of Gly or Ala respectively as the 13th amino acid, we asked whether this could be due to substrate promiscuity of the A-domain related to presence of Tyr rather than Trp at position 290 of the active site. This was further suggested by sequence analysis, which revealed that the active sites of all other Gly-only activating A-domains in relacidine, laterocidine, and brevicidine (Fig. 3A) also contain a Trp rather than a Tyr residue at position 290. To investigate this further, the 3D protein structures of all Gly-recognizing A-domains encoded by the relacidine, laterocidine, and brevicidine BGCs were first predicted with AlphaFold2. We next investigated how the Gly or Ala substrates, corresponding to relacidine A and B respectively, would fit into the A-domain active sites.[13] Based on this analysis, we hypothesize that in domains that exclusively incorporate Gly, Trp serves as a "gatekeeper" by effectively limiting the size of the active site pocket so that only the Gly substrate can fit. When modeling the corresponding Ala substrate into the active sites, the predicted distance between the Trp side chain of Gly-exclusive domains and the Ala methyl group is 1.9-2.4Å, which would likely cause steric repulsion (Fig. 3B; Supplemental Table S1). In contrast, if the A-domain active site contains the smaller Tyr residue at position 290 (as observed for the 13th A-domain encoded by the relacidine BGC) it appears to tolerate recognition of the Ala substrate, with a predicted distance of 3.4Å between the Tyr side chain and the Ala methyl group. These findings suggest that a single substitution in the active site of an A-domain can lead to substrate promiscuity, resulting in the production of NRPs with varying structural features encoded by the same BGC.

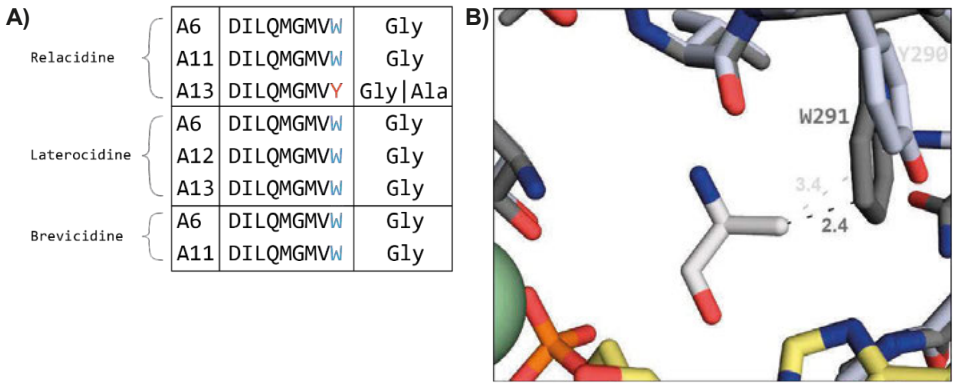

Figure 3. Comparison of the Gly-recognizing A-domains in the relacidine, laterocidine, and brevicidine biosynthetic gene clusters. A) Comparison of the active sites of the Gly-recognizing A-domains; **B)** Comparison of the 3-D structures predicted for the active sites of A-domain 13 containing Trp (laterocidine BGC; dark grey) or Tyr (relacidine BGC; grey), showing interactions of these residues with the Ala substrate.

Based on the stereochemical predictions generated from our analysis of the relacidine BGC, we next set out to synthesize relacidine A and B. The approach used was inspired by our earlier work on the total synthesis of brevicidine and laterocidine with some key differences.[8,14] Specifically, our previous solid phase peptide synthesis (SPPS) based preparation of laterocidine made use of the fact that the laterocidine macrocycle includes an Asn residue at position 11 which presented a viable option for resin attachment. However, because the relacidines lack an Asn residue at position 11, a different resin anchoring strategy was required. Instead, we identified the Ser at position 12 of the relacidine macrocycle as a viable option for resin attachment. To this end, the free sidechain hydroxyl of Fmoc-L-Ser-OAllyl was first attached to 2-chlorotrityl resin (2-CT) via an overnight coupling, which resulted in an acceptable loading of 0.37 mmol/g. The peptide was then extended to the pentapeptide using standard SPPS with the notable incorporation of Thr9 as the side-chain unprotected species (Scheme 1A). At this stage the required ester linkage between the Thr9 side chain hydroxyl and the C-terminal carboxylate of Gly13 was introduced by coupling Alloc-Gly using an on-resin Steglich esterification. After the subsequent simultaneous removal of the allyl and Alloc protecting groups, the macrocycle was formed using a BOP/DIPEA mediated amide bond formation between Ser12 and Gly13. The remaining exocyclic peptide was then elongated through eight additional rounds of SPPS, including an N-terminal lipidation using racemic 4-methylhexanoic acid. Cleavage of the peptide from resin with concomitant global deprotection was achieved using acidic conditions after which RP-HPLC purification afforded the desired relacidine A diastereomer **3a**. The same route was then applied to the synthesis of relacidine B diastereomer **4a** with the only difference being that Alloc-L-Ala was instead used to install the ester linkage with Thr9. Given that the relacidines differ from laterocidine only at positions 12 and 13, we also opted to prepare the full suite of possible relacidine A and B diastereomers based on L/D-Ser at position 12 and Gly or L/D-Ala at position 13 (Scheme 1B).

With access to relacidine A diastereomers **3a,b** and relacidine B diastereomers **4a-d** via chemical synthesis, we next set out to confirm the stereochemical configuration of the natural products by comparison with the relacidines obtained from fermentation of the producing strain. To do so, the relacidines were extracted from the cellular fraction of a *B. laterosporus* MG64 culture fermented in LB broth for 24 h. The crude extract thus obtained was analyzed using liquid chromatography-mass spectrometry (LC-MS) in order to compare the retention times of the natural and synthetic relacidines. Co-elution studies clearly demonstrated that the retention times of relacidine A and B from the bacterial extracts matched compounds **3a** and **4a**, respectively (Fig. 4). These findings support an L-configuration for Ser12 in relacidine A and B and an L-configuration for Ala13 in relacidine B, in accordance with the predictions based on our assessment of the BGC. Furthermore, analysis of the ^{1}H-NMR spectra of relacidine B diastereomers **4a-4d** (Supplemental Fig. S1) clearly show that the spectra obtained for diastereomer **4a** match the data previously published for relacidine B[9] (note: due to the extremely low isolated yield of relacidine A from fermentation, no NMR data were reported for the natural product which prevented comparison with our synthetic relacidine A diastereomers).

With the structures of relacidine A and B established, we next explored the synthesis of a relacidine A analogue wherein the ester linkage of the macrolactone ring was replaced by the corresponding amide. Our interest in this "relacidamide" analogue was two-fold: first, we

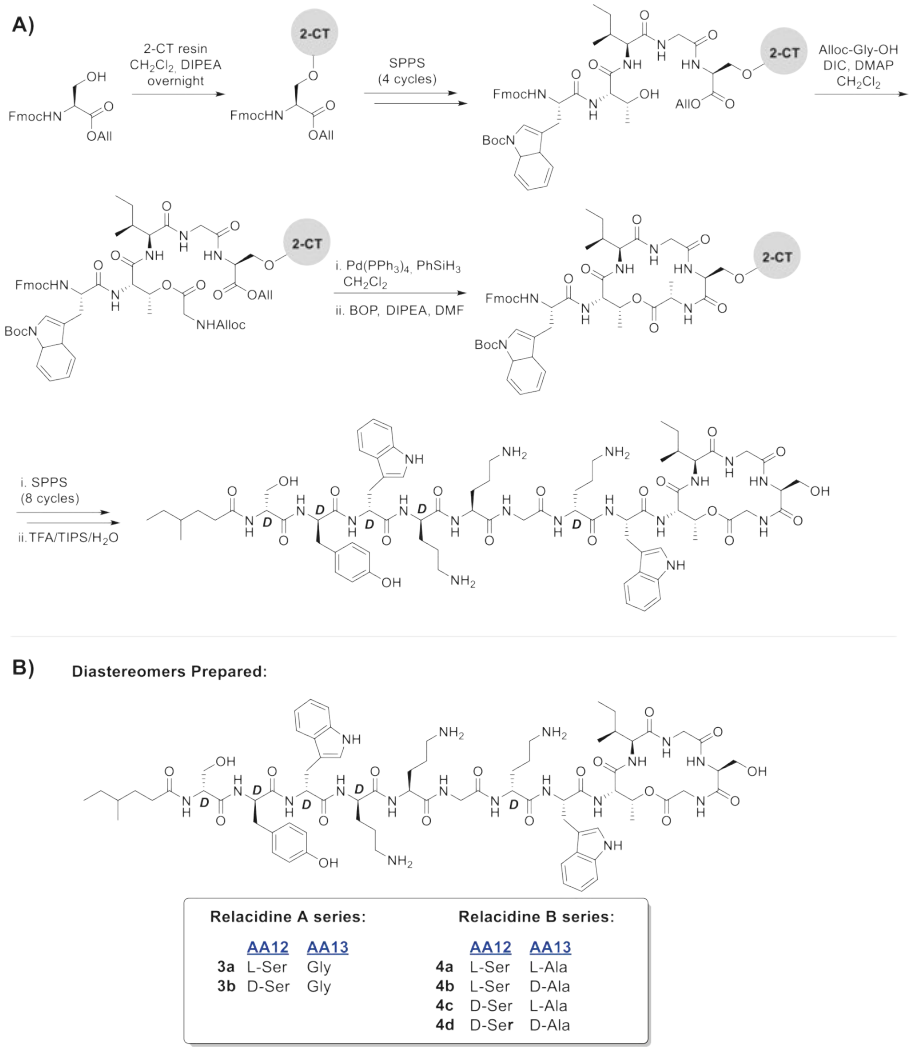

Scheme 1. A) Representative total SPPS of relacidine A (**3a**) and **B)** structures of various diastereomers of relacidine A and B also prepared.

hypothesized that the amide analogue would be more readily synthesized and second, that the macrolactam ring would be more stable to hydrolysis than the corresponding macrolactone. The synthesis of relacidamide (**5**) is depicted in Scheme 2 and was inspired by our previous work with laterocidine and brevicidine analogues.[8] Using SPPS the linear precursor peptide was assembled on 2-CT resin with the notable introduction of 3-azido-L-alanine at position 9 instead of Thr. Notably, our initial approach involved the incorporation of Alloc-L-diaminopropionic acid at position 9, however, the required on-resin deprotection of the Alloc group following completion of the linear precursor peptide was found to proceed very sluggishly. By comparison, reduction of the azide in the 3-azido-L-alanine containing peptide

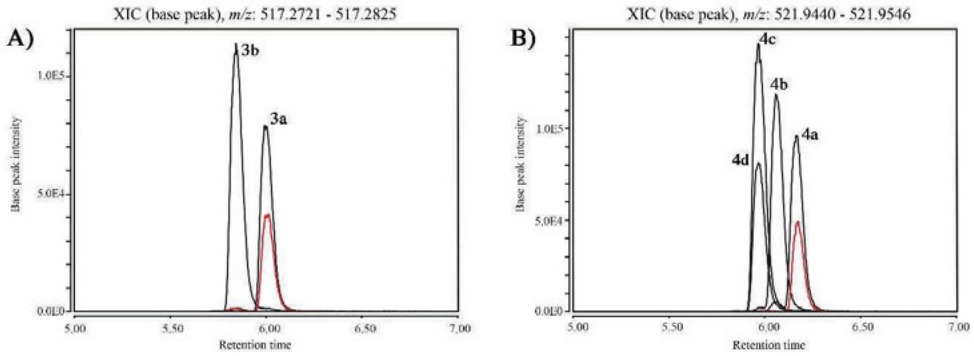

Figure 4. Extracted ion chromatograms (EICs) of: **A)** relacidine A with *m/z* 517.2776 and **B)** relacidine B with *m/z* 521.9492 from the crude extracts of *B. laterosporus* (red), overlayed with traces obtained for relacidine A diastereomers **3a,b** and relacidine B diastereomers **4a-d**. Synthetically prepared **3a** and **4a** co-elute with relacidine A and B from *B. laterosporus* MG64, respectively.

proceeded smoothly upon treatment of PMe_3, affording the amine cleanly after 3 hours. The protected linear peptide was then cleaved from the resin using mild acidic condition (HFIP/DCM) and then cyclized in solution using BOP/DIPEA. Finally, global deprotection and purification using RP-HPLC afforded pure relacidamide (**5**) in 18% yield over 30 steps.

The antibacterial activities of relacidine A (**3a**) and B (**4a**) along with diastereomers **3b** and **4b-d** as well as relacidamide (**5**) were assessed using a standard microbroth dilution assay to establish minimum inhibitory concentration (MIC) values against a panel of Gram-negative bacteria (Table 1). The MIC values measured for synthetic relacidine A (**3a**) and B (**4a**) agree well with those previously published.[9] Interestingly, the unnatural diastereomers of relacidine A and B as well as the relacidamide analogue (**5**) exhibited antibacterial activities similar to the natural products. As in the case of brevicidine and laterocidine, the biological activity of the relacidines was found to be unaffected by the clinically relevant *mcr-1* type colistin resistance. Relacidine A (**3a**) and B (**4a**) as well as relacidamide (**5**) were further tested against a panel of colistin-resistant *A. baumannii* clinical isolates which confirmed their ability to prevent the

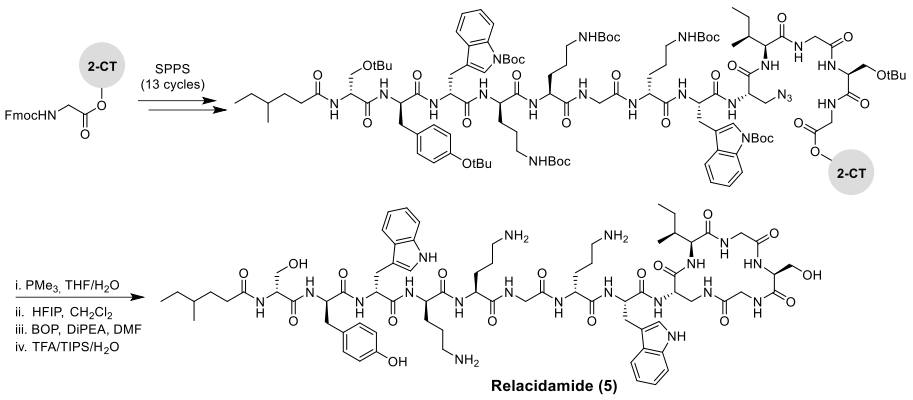

Scheme 2. Synthesis of relacidamide (**5**).

growth of colistin-resistant isolates (Supplemental Table S2). The hemolytic activity of the compounds was also assessed showing them to cause little-to-no hemolysis when tested at 128 μg/ml (Supplemental Fig. S2). Notably, while relacidine A (**3a**) showed the highest level of hemolysis at 15 % under these conditions, relacidamide analogue (**5**) showed essentially no hemolysis (1%). Also of interest was the finding that while relacidine B (**4a**) induced <1% hemolysis, substitution of either the L-Ala or L-Ser to D-Ala or D-Ser increased hemolytic activity to 8-12%. Serum stability assays were also performed revealing relacidamide (**5**) to be significantly more stable than relacidine A (**3a**), in line with expectation (Supplemental Fig. S3). LC-MS analysis indicated that the most prominent degradation product of relacidine A corresponds to the hydrolyzed species (+18 amu), presumably due to cleavage of the ester linkage between Thr9 and Gly13. Somewhat surprisingly, relacidine B (**4a**) was also found to be highly resistant to degradation in human serum even after 24h incubation. The greater hydrolytic stability of relacidine B would appear to be attributable to the increased steric bulk of the Ala sidechain next to the ester linkage (compared to the methylene of Gly in relacidine A) which may hinder the nucleophilic attack of water at the ester carbonyl.

Table 1. *In vitro* minimum inhibitory concentrations (MICs) of relacidines

	Antibacterial Activity (μg/mL)				
Peptide	***E. coli*** **ATCC 25922**	***E. coli*** **ATCC 25922 mcr-1**	***K. pneumoniae*** **ATCC 13883**	***P. aeruginosa*** **PAO1**	***S. aureus*** **USA300**
3a	2	2-4	4	4	>32
3b	2-4	4	4	2	>32
4a	1	2	4	4	>32
4b	2	2-4	4	4	>32
4c	1-2	1-2	2-4	4	>32
4d	2	2-4	2-4	8	>32
5	2-4	2-4	4	8	>32
Colistin	1	4	0.25-0.5	1	>32

Given the promising *in vitro* activity of relacidamide (**5**), along with its high serum stability, low hemolytic activity, and ease of synthesis, we further evaluated its efficacy in an established *in vivo* infection model using *G. mellonella* larvae. The *G. mellonella* infection model has gained popularity in recent years and provides a convenient method to assess the *in vivo* effectiveness and toxicity of novel antibiotics.[15,16] Relacidamide (**5**) was found to be well tolerated up to the highest tested dose after which its ability to treat infection with a colistin-resistant *A. baumannii* isolate (strain no. BV94) was assessed (Fig. 5). The larvae were first injected with either vehicle (PBS) or *A. baumannii* BV94 suspension in the right second proleg. The moth larvae were then injected in the left second proleg with either PBS (untreated), colistin at 100 mg/kg or 200 mg/kg, or relacidamide (**5**) at 100 mg/kg or 200 mg/kg. The *G. mellonella* larvae were then incubated for 72 h and their survival assessed twice per day. Relacidamide (**5**) induced 50% survival after 72 h at 100 mg/kg and 70 % survival at 200 mg/kg whereas none of the larvae treated with colistin survived and only 10 % of the untreated larvae survived after 72 h. These results also reflect the differences observed for the *in vitro* activity of relacidamide (**5**) which showed an MIC of 8 μg/ml against *A. baumannii* BV94 while colistin showed no activity at the highest concertation tested of 64 μg/ml (Supplemental Table S2).

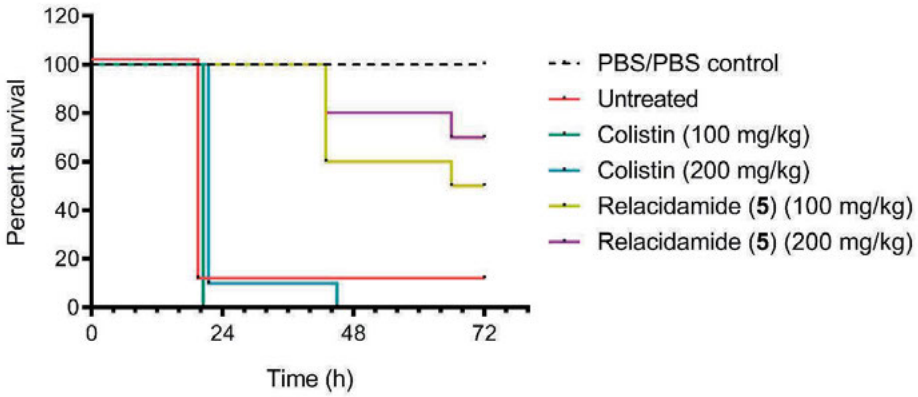

Figure 5. Percent survival of *G. mellonella* larvae after infection with colistin resistant *A. baumannii* isolate BV94 and subsequent treatment with test articles.

Conclusion

In conclusion, we here report the total synthesis of the recently discovered lipodepsipeptide antibiotics relacidine A and B, which was guided by bioinformatic analysis of the BGC. By examining the positions of the epimerization domains encoded by the relacidine BGC, we were able to predict the structure of these natural products including the stereochemical assignments of their component amino acids. Also of note, our analysis suggests that a single Trp to Tyr mutation in the active site of A-domain 13 of RlcD may allow incorporation of Ala at position 13 in relacidine B. Following on this, we developed a robust SPPS route that provided access to relacidine A and B including a number of diastereomers. Subsequent comparison of the synthetic lipopeptides with the natural products confirmed the structural predictions based on our analysis of the relacidine BGC. Furthermore, comparison of the NMR data published for relacidine B with the data obtained for the synthetic relacidine B diastereomers confirmed the predicted stereochemical configuration of relacidine B, validating our bioinformatics predictions. The antibacterial activities of the synthetic relacidines prepared, including the amide-for-ester relacidamide analogue, were evaluated against a panel of Gram-negative bacteria. All of the relacidines exhibited similar antibacterial potency while also exhibiting low hemolytic activity. In line with expectation, the relacidamide analogue (**5**) exhibited high serum stability, while retaining potent activity in *vitro*, and was therefore further evaluated *in vivo* in a *G. mellonella* larvae infection model. The compound was well tolerated at the highest dose tested and exhibited efficacy against a colistin-resistant *A. baumannii* isolate. These results showcase the relacidines as promising new lipopeptide antibiotics and indicate that further studies to more fully assess their therapeutic potential may be warranted.

Experimental Methods

Bioinformatics

We extracted the A-domains from the relacidine, laterocidine and brevicidine BGCs with HMMer (3.3.2) (http://hmmer.org), using the AMP-binding domain profile hidden Markov model (HMM) also used by antiSMASH:

https://github.com/antismash/antismash/blob/master/antismash/detection/hmm_detection/data/AMP-binding.hmm

We extracted the active sites of these A-domains and predicted their substrates using PARAS (v0.0.1; unpublished; code available at https://pypi.org/project/paras/). We predicted the structures of the Gly-recognizing A-domains of the relacidine, laterocidine and brevicidine BGCs (Table S1) with AlphaFold2, building separate structure models for the N-terminal A-subdomain and the C-terminal A-subdomain. In pymol, we combined the predicted subdomains into complete structures by aligning them to the PDB structure 1AMU, a published X-ray crystallography structure of an A-domain bound to its substrate phenylalanine. We positioned the alanine in the active site of the predicted A-domain structures by mutating the phenylalanine substrate in 1AMU to alanine and measured the distance between the alanine residue and W291/Y290 (or equivalent) with pymol's measurement wizard (Table 2).

Table 2. Distances between the modelled alanine substrate and residue 290 based on AlphaFold structure models. The domains visualized in Fig. 3B are indicated in bold.

Domain	Module nr	Residue at position 290 or equivalent	Distance between Ala substrate and residue 290
RlcC A6	6	W290	1.9Å
RlcD A2	11	W294	2.4Å
RlcD A4	**13**	**Y290**	**3.4Å**
LatC A6	6	W290	2.5Å
LatD A3	12	W297	2.2Å
LatD A4	**13**	**W291**	**2.4Å**
BreC A6	6	W290	2.3Å
BreD A2	11	W297	2.4Å

Materials

All reagents employed were of American Chemical Society (ACS) grade or higher and were used without further purification unless otherwise stated. Fmoc-L-Ser-OAllyl and Fmoc-D-Ser-OAllyl[17] as well as Alloc-Gly-OH, Alloc-L-Ala-OH and Alloc-D-Ala-OH[18] were synthesized according to referenced literature procedures. Fmoc-L-Orn(Boc)-OH, Fmoc-D-Orn(Boc)-OH and 4-methylhexanoic acid were purchased from Combi-Blocks. All other Fmoc-amino acids were purchased from P3 BioSystems. 2-Chloro trityl chloride (2-CT) resin was purchased from Iris Biotech. ((1H-Benzo[d][1,2,3]triazol-1-yl)oxy)tris(dimethylamino) phosphonium hexafluorophosphate (BOP), N,N-Diisopropylcarbodiimide (DIC) and triisopropylsilane (TIPS) were purchased from Manchester Organics. 1M PMe_3 in THF and 4-Dimethylaminopyridine (DMAP) were purchased from Sigma Aldrich. Phenylsilane

was purchased from Thermo Scientific ($PhSiH_3$). Fmoc-L-azidoalanine was purchased from Chiralix. Diisopropylethylamine (DIPEA), piperidine, trifluoroacetic acid (TFA) and dimethyl sulfoxide (DMSO) were purchased from Carl Roth. Dichloromethane (CH_2Cl_2) and petroleum ether were purchased from VWR Chemicals. Acetonitrile (MeCN), dimethylformamide (DMF) and methyl tertiary-butyl ether (MTBE) were purchased from Biosolve.

General procedures for peptide synthesis

Resin Loading

2-Chlorotrityl chloride resin (2-CT) (5 g, 1.55 mmol/g) was loaded by overnight coupling via the free sidechain hydroxyl of Fmoc-L-Ser-OAllyl (2.84 g, 7.75 mmol, 1 eq.) or Fmoc-D-Ser-OAllyl (1.5 g, 7.75 mmol, 1 eq.) with DIPEA (1.4 mL, 7.75 mmol, 1 eq.) in 23 mL of CH_2Cl_2. The suspension was stirred under argon at 45°C for 5 min. An additional volume of DIPEA (2.1 mL, 11.1 mmol, 1.5 eq.) was added, the suspension was stirred under argon at 45°C, overnight. After capping with MeOH (0.92 mL, 22.7 mmol, 3 eq.) and DIPEA (0.67 mL, 3.7 mmol, 0.5 eq.) for 15 min, the resin was filtered, washed and dried overnight under a stream of air. The resin loading was then determined to be 0.37 mmol/g and 0.33 mmol/g for 2-CT-Fmoc-L-Ser-OAllyl and 2-CT-Fmoc-D-Ser-OAllyl respectively.

Synthesis of Relacidines (3a-4d)

Resin loaded with Fmoc-L-Ser-OAllyl (0.68 g, 0.25 mmol) or Fmoc-D-Ser-OAllyl (0.75 g, 0.25 mmol) was added to a manual SPPS cartridge and bubbled with nitrogen in DMF (5 mL, 30 min) to swell. Fmoc deprotections (1 min then 10 min) were carried out with 5 mL of dry piperidine in DMF (1 : 5, v/v). The next 4 amino acids (Gly11, Ile10, Thr9, Trp8) were coupled manually (1 h) under nitrogen flow via standard Fmoc solid-phase peptide synthesis (SPPS) (resin : Fmoc-AA : BOP : DIPEA, 1 : 4 : 4 : 8 molar eq.). The following Fmoc amino acids were used: Fmoc-Gly-OH, Fmoc-Ile-OH, Fmoc-Thr-OH (used without sidechain protection) and Fmoc-Trp(Boc)-OH. After coupling of Fmoc-Trp(Boc)-OH, esterification of the Thr sidechain was achieved by treating the resin-bound peptide with Alloc-Gly-OH (0.60 g, 3.75 mmol, 15 eq.), DIC (0.59 mL, 3.75 mmol, 15 eq.), and DMAP (15 mg, 0.13 mmol, 0.5 eq.) in 8 mL CH_2Cl_2 : DMF (3 : 1, v/v) for 18 h under argon, for relacidine A; or Alloc-L-Ala-OH or Alloc-D-Ala-OH (0.65 g, 3.75 mmol, 15 eq.), DIC (0.59 mL, 3.75 mmol, 15 eq.), and DMAP (15 mg, 0.13 mmol, 0.5 eq.) in 8 mL CH_2Cl_2 : DMF (3 : 1, v/v) for 18 h under argon, for relacidine B. The resin was treated with $Pd(PPh_3)_4$ (75 mg, 0.075 mmol, 0.3 eq.), and $PhSiH_3$ (0.75 mL, 7.5 mmol, 30 eq.) in CH_2Cl_2 (16.5 mL) under argon for 2 h. The resin was subsequently washed with dry CH_2Cl_2 (5 x 5 mL x 3 min), diethyldithiocarbamic acid trihydrate sodium salt in dry DMF (5 mg/mL, 5 x 5 mL x 3 min), and dry DMF (5 x 5 mL x 3 min). Subsequently, BOP (442 mg, 1.0 mmol, 4 eq.) and dry DIPEA (0.35 mL, 2.0 mmol, 8 eq.) were added to cyclize the peptide in 5 mL of DMF, the suspension was bubbled with nitrogen for 1 h. The remaining N-terminal section of the peptide was then synthesized using the standard SPPS protocol mentioned above. The following Fmoc amino acids were used: Fmoc-D-Orn(Boc)-OH, Fmoc-Gly-OH, Fmoc-L-Orn(Boc)-OH, Fmoc-D-Trp(Boc)-OH, Fmoc-D-Tyr(tBu)-OH, and Fmoc-D-Ser(tBu)-OH. Following the coupling of the last amino acid, the resin was split into two batches of 0.125 mmol. 4-Methylhexanoic acid (34 mg, 0.25 mmol, 2 eq.) was coupled using BOP (221 mg, 0.5 mmol, 4 eq.), and DIPEA (0.17 mL, 1.0 mmol, 8 eq.) in dry DMF (3 mL), under nitrogen flow for 2 h. Final deprotection was carried

out by treating the resins with TFA : H_2O : TIPS (95 : 2.5 : 2.5, v/v, 5 mL) for 90 min while shaking. The reaction mixture was filtered through cotton, the filtrate was precipitated from MTBE : petroleum ether (1 : 1, v/v, 45 mL) and centrifuged (4500 rpm, 5 min). The pellet was then resuspended in MTBE : petroleum ether (1 : 1, v/v, 50 mL) and centrifuged again (4500 rpm, 5 min). Finally the pellet containing the crude lipopeptide was dissolved in tBuOH : H_2O (1 : 1, v/v, 20 mL) and lyophilized overnight. The crude mixtures were subsequently purified by RP-HPLC (See Purification and analysis methods). Fractions were assessed by HPLC and LC-MS and product containing fractions were pooled, frozen and lyophilized to yield the pure lipopeptides as white powders in 3–10% yield over 28 steps. See section V, HPLC and HRMS analysis of peptides, for traces and individual yields.

Synthesis of Relacidamide (5)

2-Chlorotrityl resin (2-CT) (5.0 g, 1.60 mmol/g) was loaded with 1 eq. Fmoc-Gly-OH following the same protocol as described above. Resin loading was determined to be 0.67 mmol/g. The linear peptide was assembled manually on a 0.25 mmol scale under nitrogen flow via standard Fmoc solid-phase peptide synthesis (SPPS) (1 h couplings, resin : Fmoc-AA : BOP : DIPEA, 1 : 4 : 4 : 8 molar eq.). DMF (5 mL) was used as solvent and Fmoc deprotections (5 min then 15 min) were carried out with 5 mL piperidine : DMF (1 : 4, v/v). The following Fmoc amino acids were used: Fmoc-D-Ser(tBu)-OH, Fmoc-D-Tyr(tBu)-OH, Fmoc-D-Trp(Boc)-OH, Fmoc-D-Orn(Boc)-OH, Fmoc-L-Orn(Boc)-OH, Fmoc-Gly-OH, Fmoc-Trp(Boc)-OH, Fmoc-L-azidoalanine, Fmoc-Ile-OH and Fmoc-Ser(tBu)-OH. Following the final Fmoc removal step, 4-methylhexanoic acid (65 mg, 0.5 mmol, 2 eq.) was coupled using BOP (221 mg, 0.5 mmol, 2 eq.) and DIPEA (0.17 mL, 1.0 mmol, 4 eq.) in 5 mL of DMF overnight, under nitrogen flow. The azide was reduced by treating the resin with 9 mL of 1M PMe_3 in THF and 1 mL of H_2O for 3 hours. After washing the resin with DMF and CH_2Cl_2, the peptide was cleaved off the resin by treating it with HFIP : CH_2Cl_2 (1 : 4, v/v, 20 mL) for 1 hour and rinsed with additional HFIP : CH_2Cl_2 and CH_2Cl_2. The combined washings were then evaporated to yield the linear protected peptide with a free C-terminus and amino sidechain. The peptide was dissolved in 250 mL of CH_2Cl_2 and 50 mL of DMF, treated with BOP (221 mg, 0.5 mmol, 2 eq.) and DIPEA (0.17 mL, 1.0 mmol, 4 eq.) and the solution was stirred overnight under nitrogen atmosphere. The reaction mixture was concentrated *in vacuo* and directly treated with TFA : H_2O : TIPS (95 : 2.5 : 2.5, v/v, 10 mL) for 90 min while shaking. The reaction mixture was filtered through cotton, the filtrate was precipitated from MTBE : petroleum ether (1 : 1, v/v, 45 mL) and centrifuged (4500 rpm, 5 min). The pellet was then resuspended in MTBE : petroleum ether (1 : 1, v/v, 50 mL) and centrifuged again (4500 rpm, 5 min). Finally the pellet containing the crude lipopeptide was dissolved in tBuOH : H_2O (1 : 1, v/v, 20 mL) and lyophilized overnight. The crude mixture were subsequently purified by RP-HPLC (See Purification and analysis methods). Fractions were assessed by HPLC and LC-MS and product containing fractions were pooled, frozen and lyophilized to yield the pure lipopeptide as white powder in 18% yield over 30 steps.

Purification and analysis methods

Preparative HPLC: Purification was performed on a BESTA-Technik system with a Dr. Maisch ReproSil Gold 120 C18 column (10 µm, 25 x 250 mm) and equipped with a ECOM Flash UV detector. Runs were performed at a flow rate of 12 mL/min with UV detection at 214 nm and 254 nm. Solvent A = 0.1% TFA in water/MeCN (95 : 5) and solvent B = 0.1%

TFA in water/MeCN (5 : 95). A gradient method was employed, starting at 100 % solvent A for 2 min, ramping up to 100 % solvent B over 55 min, remaining at 100 % solvent B for 3 min before ramping down to 100 % solvent A over 1 min and remaining there for 1 min. Product containing fractions were pooled, partially concentrated under vacuum, frozen and then lyophilized to yield pure peptides as white flocculent solids. A small amount of purified peptide was analyzed by analytical HPLC.

Analytical HPLC: Analytical runs were performed on a Shimadzu Prominence-i LC-2030 system with a Dr. Maisch ReproSil Gold 120 C18 (5 µm, 4.6 x 250 mm) at 30 °C. Runs were performed at a flow rate of 1 mL/min with UV detection at 214 nm and 254 nm. Solvent A = 0.1% TFA in water/MeCN (95 : 5) and solvent B = 0.1% TFA in water/MeCN (5 : 95). A gradient method was employed, starting at 100% solvent A for 2 min, ramping up to 50 % solvent B over 23 min, ramping up to 100% solvent B over 1 min, remaining there for 2 min before ramping down to 100% solvent A over 1 min and remaining there for 1 min.

HRMS: HRMS spectra were acquired on a Thermo Scientific Dionex UltiMate 3000 HPLC system with a Phenomenex Kinetex C18 (2.6 µm, 2.1 x 150 mm) column at 35 °C and equipped with a diode array detector. The following solvent system, at a flow rate of 0.3 mL/min, was used: solvent A = 0.1% formic acid in water, solvent B = 0.1% formic acid in MeCN. A gradient method was employed, starting at 95 % solvent A and 5 % solvent B for 1 min, ramping up to 95 % solvent B over 9 min, ramping up to 98 % solvent B over 1 min, remaining there for 1 min before ramping back down to 95 % solvent A over 2 min and remaining there for 1 min. The system was connected to a Bruker micrOTOF-Q II mass spectrometer (ESI ionization) calibrated internally with sodium formate.

Culturing conditions and extraction of natural products

Brevibacillus laterosporus MG64 was cultured on Luria-Bertani (LB) agar and colonies grown overnight in 5 ml LB broth at 37°C. This inoculum was transferred to 2 L Erlenmeyer flasks containing 500 ml of LB broth and incubated at 37°C with 220 rpm shaking for 24 h. Cells were collected by centrifugation (10,000 × *g*, 10 min, 4°C) and extracted with 100 mL of 70% isopropyl alcohol (IPA), pH 2 (acidified with 1 M HCl). Supernatant was separated by centrifugation (6000×g, 10 min, 4 °C) and solvent was evaporated under vacuum using rotary evaporation. The crude extract was reconstituted in H_2O and filtered with a 0.22 µm syringe filter.

LC–MS/MS analysis

LC–MS analysis was performed using a Shimadzu Nexera X2 UHPLC system coupled to a Shimadzu 9030 QTOF mass spectrometer as previously described.[19] Briefly, extracts and pure compounds were dissolved in H_2O to a final concentration of 1 mg/mL and 0.01 mg/mL, and 2 µL was injected into a Waters Acquity HSS C18 column (1.8 µm, 100 Å, 2.1 × 100 mm). The column was maintained at 30 °C, and run at a flow rate of 0.5 mL/min, using 0.1% formic acid in water as solvent A, and 0.1% formic acid in MeCN as solvent B. A gradient was employed for chromatographic separation starting at 5% B for 1 min, then 5 – 85% B for 9 min, 85 – 100% B for 1 min, and finally held at 100% B for 4 min. The column was re-equilibrated to 5% B for 3 min before the next run was started. The parameters used for the ESI source were:

interface voltage 4 kV, interface temperature 300 °C, nebulizing gas flow 3 L/min, and drying gas flow 10 L/min.

Antimicrobial testing

Table 3. Minimum inhibitory concentrations (MICs) determined against panel of previously characterized colistin-resistant *A. baumannii* clinical isolates[20]

	Antibacterial Activity (μg/mL)			
Strain	**Relacidine A (3a)**	**Relacidine B (4a)**	**Relacidamide (5)**	**Colistin**
***A. baumannii* ATCC 17978**	8	4	4	1
***A. baumannii* NCTC 13304**	4	4	4	1
***A. baumannii* NCTC 13420**	8	16	16	0.5
***A. baumannii* HUMC1**	16	8	8	1
***A. baumannii* LAC-4**	4	8	8	0.5
***A. baumannii* BV94**	8	16	8	>64
***A. baumannii* BV95**	8	8	8	32
***A. baumannii* BV172**	16	16	16	>64
***A. baumannii* BV173**	8	16	16	16

Colistin sulfate was purchased from Activate Scientific. Kanamycin monosulfate was purchased from MP Biomedicals. *E. coli* ATCC 25922, *S. aureus* USA300 (ATCC BAA1717) and *K. pneumoniae* ATCC 13883 belong to the American Type Culture Collection (ATCC). *P. aeruginosa* PAO1 was kindly provided by L.H.C. Quarles Van Ufford, Utrecht University, Utrecht, The Netherlands. *E. coli* ATCC 25922 MCR-1 was transfected in house using the pGDP2-MCR1 plasmid kindly provided by Yong-Xin Li, The University of Hong Kong, Hong Kong, China. Sheep blood agar plates (Ref. PB5039A) were purchased from Thermo Scientific. Tryptic soy broth (Ref. 02-200-500) was purchased from Scharlab. Mueller-Hinton broth (Ref. X927.1) was purchased from Carl Roth. Polypropylene 96-wells plates (Ref. 3879) were purchased from Corning.

All minimum inhibitory concentrations were determined according to Clinical and Standards Laboratory Institute (CLSI) guidelines. Blood agar plates were inoculated from glycerol stocks of the different *A. baumannii* strains used and then incubated for 16 h at 37 °C. Individually grown colonies were subsequently used to inoculate 5 mL aliquots of TSB that were then incubated at 37 °C. In parallel, the lipopeptide antibiotics DMSO stocks to be assessed were serially diluted with cation-adjusted MHB in polypropylene 96-well plates (50 μL in each well). Colistin sulfate stocks were dissolved in water before being diluted with cation-adjusted MHB. The *A. baumannii* inoculated TSB aliquots were incubated until an OD_{600} of around 0.5 was reached. The bacterial suspensions were then diluted with cation-adjusted MHB (2×10^5 CFU mL^{-1}) and added to the microplates containing the test compounds (50 μL to each well). The well-plates were sealed with an adhesive membrane and after 18 h of incubation at 37 °C visually inspected for bacterial growth. MIC values reported are based on three technical replicates and defined as the lowest concentration of the compound that prevented visible growth of bacteria.

Hemolytic assay

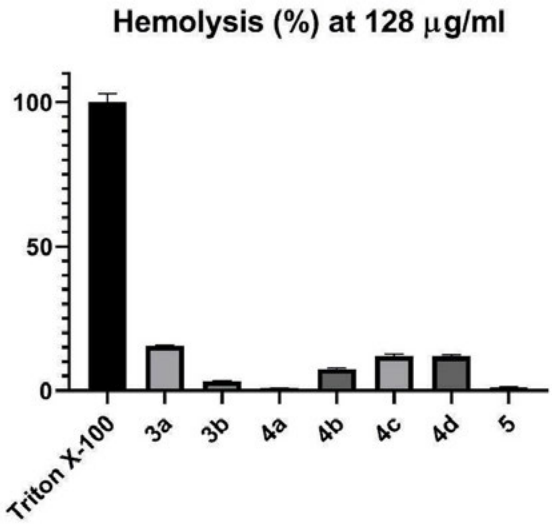

Figure 6. Hemolytic activity of compounds **3a-5** at 128 μg/mL and 1 h incubation against sheep red blood cells. Colistin was also included as a reference and showed no detectable hemolysis (<0.1%) under the same conditions.

Experiments were performed in triplicate and Triton X-100 used as a positive control. Red blood cells from defibrinated sheep blood obtained from Thermo Fisher were centrifuged (400 g for 15 min at 4°C) and washed with Phosphate-Buffered Saline (PBS) containing 0.002% Tween20 (buffer) five times. Then, the red blood cells were normalized to obtain a positive control read-out between 2.5 and 3.0 at 415 nm to stay within the linear range with the maximum sensitivity. A serial dilution of the compounds (128 – 1 μg/mL, 75 μL) was prepared in a 96-well polypropylene plate. The outer border of the plate was filled with 75 μL buffer. Each plate contained a positive control (0.1% Triton-X final concentration, 75 μL) and a negative control (buffer, 75 μL) in triplicate. The normalized blood cells (75 μL) were added and the plates were incubated at 37 °C for 1 h while shaking at 500 rpm. A flat-bottom polystyrene plate with 100 μL buffer in each well was prepared. After incubation, the plates were centrifuged (800 g for 5 min at room temperature) and 25 μL of the supernatant was transferred to their respective wells in the flat-bottom plate. The values obtained from a read-out at 415 nm were corrected for background (negative control) and transformed to a percentage relative to the positive control.

Serum Stability assay

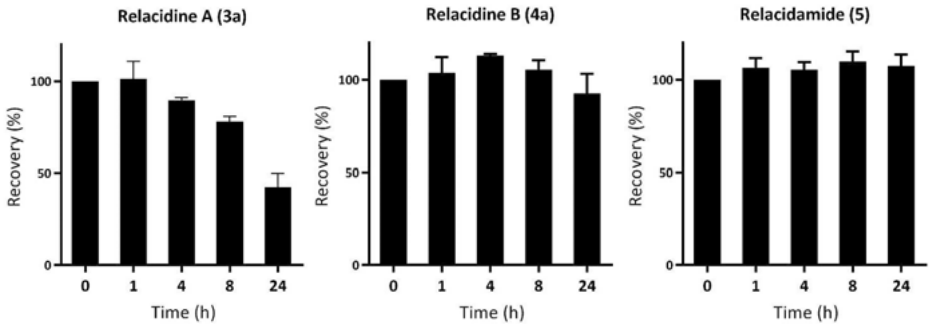

Figure 7. Serum stability assay comparing natural lipopeptides **3a** and **4a** to relacidamide analogue **5**.

10 mg/mL peptide solutions were prepared in in Milli-Q water. Samples were prepared with 42 µL peptide solution and 518 µL human serum (obtained from Sigma Aldrich, product number: H4522) and incubated at 37 °C. Samples were taken at t = 0, 1, 4, 8 and 24 h. To 100 µL of serum, 100 µL of 6% trichloroacetic acid in acetonitrile (containing 0.2 µg/mL D-Phenylalanine as internal standard) was added to precipitate the proteins. The samples were vortexed, left for 15 min at room temperature and stored at -20 °C. Before analysis the samples were centrifuged for 5 min at 13 000 rpm. The supernatant was analyzed by RP-HPLC using a Shimadzu Prominence-i LC-2030 system with a Dr. Maisch ReproSil Gold 120 C18 column (4.6 × 250 mm, 5 µm) at 30 °C and equipped with a UV detector monitoring at 220 nm and 254 nm. The following solvent system, at a flow rate of 1 mL/min, was used: solvent A, 0.1 % TFA in water/acetonitrile 95/5; solvent B, 0.1 % TFA in water/acetonitrile 5/95. Gradient elution was as follows: 100:0 (A/B) for 2 min, 100:0 to 50:50 (A/B) over 45 min, 50:50 (A/B) to 0:100 (A/B) over 1 min, 0:100 (A/B) for 6 min then reversion back to 100:0 (A/B) over 1 min, 100:0 (A/B) for 5 min. The peaks were integrated and normalized to the internal standard. The t=0 value was then set at 100% for each analogue and all time-points were calculated as a percentage of t=0. Biological duplicates of the experiment were performed.

***In vivo* experiments**

Ten *G. mellonella* larvae (Serum Therapeutics Inc., average weight 0.265 g) per group were infected using a 10-µl injection in the right second proleg with mid-log phase (OD_{600} = 0.5) growing bacteria resuspended and diluted in phosphate-buffered saline (PBS) to achieve the target inoculum of 10^5 colony forming unit (cfu) per larva. Inoculum density was verified by plating suitable dilutions on non-selective Luria-Bertani agar. Treatment was performed at 1 hour post-infection by injecting 10 µl of the indicated compound dose in the left second proleg. The infected larvae were collected in a Petri dish and incubated at 37°C. The viability of the larvae was assessed twice a day up to a total of 72 hours post-infection by checking for movement. Larvae were considered dead if no movement could be observed in response to stimulus with a pipette tip.

HPLC and HRMS analysis of peptides

Table 4. Peptide number, name, chemical formula, exact mass, mass found and overall yield for peptides **3a**-**5**. HPLC traces of the peptides can be found in the online supplementary material at DOI https://doi.org/10.1021/acsinfecdis.3c00043

Compound	Name	Chemical Formula	Calcd Exact Mass	Mass found	Calcd	Overall Yield [%]
3a	Relacidine A	$C_{75}H_{108}N_{18}O_{18}$	1548.8089	775.4117	775.4118	5.4
3b	D-Ser12-Relacidine A	$C_{75}H_{108}N_{18}O_{18}$	1548.8089	775.4120	775.4118	6.8
4a	Relacidine B	$C_{76}H_{110}N_{18}O_{18}$	1562.8245	782.4199	782.4195	9.1
4b	D-Ala13, L-Ser12-Relacidine B	$C_{76}H_{110}N_{18}O_{18}$	1562.8245	782.4197	782.4195	9.5
4c	L-Ala13, D-Ser12-Relacdine B	$C_{76}H_{110}N_{18}O_{18}$	1562.8245	782.4199	782.4195	3.2
4d	D-Ala13, D-Ser12-Relacdine B	$C_{76}H_{110}N_{18}O_{18}$	1562.8245	782.4195	782.4195	5.7
5	Relacidamide	$C_{74}H_{107}N_{19}O_{17}$	1533.8092	767.9120	767.9119	18

NMR characterization

Table 5. ^{1}H-NMR (d_6-DMSO) characterization of relacidine A (**3a**)

Residue	-NH	Hα	Hβ	Hγ	Hδ	Hε
D-Ser1	7.88 (1H, d, *J* = 7.4 Hz)	4.27 (1H, m)	3.51 (2H, m)	5.11 (1H, t, *J* = 5.4 Hz)		
D-Tyr2	8.01 (1H, m)	4.36 (1H, m)	2.83 (1H, dd, *J* = 14.2, 4.3 Hz) & 2.62 (1H, m)	Phenol: 9.17 (1H, s), 6.89 (2H, d, *J* = 8.5 Hz), 6.57 (2H, d, *J* = 8.5 Hz)		
D-Trp3	8.00 (1H, m)	4.52 (1H, m)	3.17 (1H, m) & 2.95 (1H, m)	Indole: 10.79 (1H, s), 7.57 (1H, d, *J* = 7.9 Hz), 7.34 (1H, d, *J* = 8.1 Hz), 7.15 (1H, d, *J* = 2.3 Hz), 7.07 (1H, m)), 6.99 (1H, t, *J* = 7.2 Hz)		
D-Orn4	8.04 (1H, d, *J* = 8.1 Hz)	4.38 (1H, m)	1.73 (1H, m) & 1.56 (1H, m)	1.56 (2H, m)	2.78 (2H, m)	7.69 (2H, br m)
Orn5	8.08 (1H, d, *J* = 8.1 Hz)	4.41 (1H, m)	1.71 (1H, m) & 1.53 (1H, m)	1.53 (2H, m)	2.77 (2H, m)	7.69 (2H, br m)
Gly6	8.26 (1H, m)	3.83 (1H, m) & 3.73 (1H, m)				
D-Orn7	8.11 (1H, m)	4.38 (1H, m)	1.40 (1H, m) & 1.28 (1H, m)	1.33 (2H, m)	2.59 (2H, m)	7.62 (2H, br m)
Trp8	8.18 (1H, d, *J* = 8.2 Hz)	4,76 (1H, m)	3.13 (1H, dd, *J* = 14.5, 5.1 Hz) & 2.95 (1H, m)	Indole: 10.77 (1H, s), 7.57 (1H, d, *J* = 7.9 Hz), 7.31 (1H, d, *J* = 8.1 Hz), 7.09 (1H, d, *J* = 2.4 Hz), 7.04 (1H, m), 6.95 (1H, t, *J* = 7.2 Hz)		
Thr9	8.08 (1H, d, *J* = 8.1 Hz)	4.58 (1H, dd, *J* = 8.3, 4.1 Hz)	4.96 (1H, m)	1.02 (3H, d, *J* = 6.6 Hz)		
Ile10	7.95 (1H, d, *J* = 9.2 Hz)	4.27 (1H, m)	1.67 (1H, m)	1.50 (1H, m) & 1.10 (1H, m), 0.84 (3H, d, *J* = 6.8 Hz)	0.86 (3H, t, *J* = 7.4 Hz)	
Gly11	9.19 (1H, t, *J* = 5.1 Hz)	3.94 (1H, m) & 3.33 (1H, under H_2O)				
Ser12	8.56 (1H, d, *J* = 8.1 Hz)	4.12 (1H, m)	3.74 (1H, m) & 3.66 (1H, m)	4.88 (1H, t, *J* = 5.7 Hz)		
Gly13	8.12 (1H, m)	3.94 (1H, m) & 3.81 (1H, m)				
Lipid	2.12 (2H, m, O=CC**H**$_2$), 1.50 (2H, O=CCH$_2$C**H**$_2$), 1.27 (5H, -C**H**$_2$C**H**(CH)$_3$C**H**$_2$CH$_3$), 1.09 (2H, -C**H**$_2$CH$_3$), 0.82 (6H, -CH(C**H**$_3$)CH$_2$C**H**$_3$)					

Table 6. ^{1}H-NMR (d_6-DMSO) characterization of D-Ser12-relacidine A (**3b**)

Residue	-NH	Hα	Hβ	Hγ	Hδ	Hε
D-Ser1	7.89 (1H, d, *J* = 7.3 Hz)	4.27 (1H, q, *J* = 6.5 Hz)	3.51 (2H, m)	5.14 (1H, br s)		
D-Tyr2	8.02 (1H, m)	4.34 (1H, m)	2.83 (1H, dd, *J* = 14.2, 4.3 Hz) & 2.62 (1H, m)	Phenol: 9.18 (1H, s), 6.89 (2H, d, *J* = 8.6 Hz), 6.57 (2H, d, *J* = 8.4 Hz)		
D-Trp3	8.01 (1H, m)	4.52 (1H, m)	3.16 (1H, m) & 2.95 (1H, m)	Indole: 10.80 (1H, s), 7.64 (1H, m), 7.34 (1H, d, *J* = 8.1 Hz), 7.15 (1H, d, *J* = 2.4 Hz), 7.07 (1H, t, *J* = 7.5 Hz), 6.99 (1H, t, *J* = 7.4 Hz)		
D-Orn4	8.02 (1H, m)	4.38 (1H, m)	1.73 (1H, m) & 1.56 (1H, m)	1.56 (2H, m)	2.78 (2H, m)	7.75 (2H, br m)
Orn5	8.09 (1H, d, *J* = 8.4 Hz)	4.41 (1H, m)	1.71 (1H, m) & 1.53 (1H, m)	1.53 (2H, m)	2.77 (2H, m)	7.75 (2H, br m)
Gly6	8.24 (1H, t, *J* = 5.6 Hz)	3.83 (1H, m) & 3,75 (1H, m)				
D-Orn7	8.04 (1H, d, *J* = 8.5 Hz)	4.38 (1H, m)	1.36 (1H, m) & 1.20 (1H, m)	1.28 (2H, m)	2.56 (2H, m)	7.65 (2H, br m)
Trp8	8.21 (1H, d, *J* = 8.2 Hz)	4,72 (1H, m)	3.16 (1H, m) & 2.91 (1H, m)	Indole: 10.76 (1H, s), 7.57 (1H, d, *J* = 7.9 Hz), 7.31 (1H, d, *J* = 8.0 Hz), 7.14 (1H, d, *J* = 2.4 Hz), 7.04 (1H, t, *J* = 7.5 Hz), 6.96 (1H, t, *J* = 7.4 Hz)		
Thr9	7.85 (1H, d, *J* = 8.8 Hz)	4.68 (1H, dd, *J* = 8.9, 3.1 Hz)	5.19 (1H, m)	1.14 (3H, d, *J* = 6.2 Hz)		
Ile10	8.40 (1H, d, *J* = 3.7 Hz)	3.90 (1H, dd, *J* = 7.6, 3.7 Hz)	1.64 (1H, m)	1.61 (1H, m) & 1.19 (1H, m), 0.88 (3H, d, *J* = 6.8 Hz)	0.90 (3H, t, *J* = 7.3 Hz)	
Gly11	9.22 (1H, t, *J* = 5.5 Hz)	3.73 (1H, m) & 3.65 (1H, m)				
D-Ser12	7.52 (1H, t, *J* = 9.1 Hz)	4.37 (1H, m)	3.98 (1H, m) & 3.83 (1H, m)	4.87 (1H, br s)		
Gly13	7.52 (1H, t, *J* = 9.1 Hz)	4.50 (1H, m) & 3.39 (1H, under H_2O)				
Lipid	2.12 (2H, m, O=CC**H**$_2$), 1.50 (2H, O=CCH$_2$C**H**$_2$), 1.27 (5H, -C**H**$_2$C**H**(CH)$_3$C**H**$_2$CH$_3$), 1.09 (2H, -C**H**$_2$CH$_3$), 0.82 (6H, -CH(C**H**$_3$)CH$_2$C**H**$_3$)					

Table 7. ^{1}H-NMR (d_6-DMSO) characterization of relacidine B (**4a**)

Residue	-NH	Hα	Hβ	Hγ	Hδ	Hε
D-Ser1	7.88 (1H, d, *J* = 7.4 Hz)	4.27 (1H, m)	3.51 (2H, m)	5.13 (1H, br s)		
D-Tyr2	8.02 (1H, m)	4.35 (1H, m)	2.83 (1H, m) & 2.62 (1H, m)	Phenol: 9.17 (1H, m), 6.90 (2H, d, *J* = 8.5 Hz), 6.57 (2H, d, *J* = 8.4 Hz)		
D-Trp3	8.01 (1H, m)	4.52 (1H, m)	3.16 (1H, dd, *J* = 15.0, 4.5 Hz) & 2.95 (1H, m)	Indole: 10.79 (1H, s), 7.57 (1H, d, *J* = 8.0 Hz), 7.34 (1H, d, *J* = 8.1 Hz), 7.15 (1H, d, *J* = 2.4 Hz), 7.07 (1H, m), 6.99 (1H, m)		
D-Orn4	8.03 (1H, m)	4.38 (1H, m)	1.73 (1H, m) & 1.56 (1H, m)	1.56 (2H, m)	2.78 (2H, m)	7.72 (2H, br m)
Orn5	8.09 (1H, d, *J* = 8.3 Hz)	4.41 (1H, m)	1.71 (1H, m) & 1.53 (1H, m)	1.53 (2H, m)	2.77 (2H, m)	7.72 (2H, br m)
Gly6	8.26 (1H, t, *J* = 5.6 Hz)	3.84 (1H, m) & 3.74 (1H, dd, *J* = 16.9, 5.1 Hz)				
D-Orn7	8.11 (1H, d, *J* = 8.4 Hz)	4.38 (1H, m)	1.41 (1H, m) & 1.29 (1H, m)	1.34 (2H, m)	2.59 (2H, m)	7.65 (2H, br m)
Trp8	8.22 (1H, d, *J* = 8.1 Hz)	4,75 (1H, m)	3.11 (1H, dd, *J* = 14.7, 5.2 Hz) & 2.96 (1H, m)	Indole: 10.78 (1H, s), 7.59 (1H, d, *J* = 7.9 Hz), 7.31 (1H, d, *J* = 8.0 Hz), 7.11 (1H, d, *J* = 2.4 Hz), 7.04 (1H, m), 6.96 (1H, m)		
Thr9	8.06 (1H, d, *J* = 8.1 Hz)	4.64 (1H, dd, *J* = 8.1, 4.0 Hz)	5.00 (1H, m)	0.99 (3H, d, *J* = 6.5 Hz)		
Ile10	7.72 (1H, m)	4.17 (1H, t, *J* = 8.5 Hz)	1.66 (1H, m)	1.54 (1H, m) & 1.11 (1H, m), 0.86 (3H, m)	0.87 (3H, m)	
Gly11	9.17 (1H, t, *J* = 6.4 Hz)	3.91 (1H, dd, *J* = 14.3, 4.7 Hz) & 3.36 (1H, under H_2O)				
Ser12	8.46 (1H, d, *J* = 7.8 Hz)	4.10 (1H, m)	3.81 (1H, m) & 3.69 (1H, dd, *J* = 11.0, 3.4 Hz)	4.88 (1H, br s)		
Ala13	7.76 (1H, d, *J* = 8.6 Hz)	4.39 (1H, m)	1.43 (3H, d, *J* = 7.2 Hz)			
Lipid	2.12 (2H, m, O=CC**H**$_2$), 1.50 (2H, O=CCH$_2$C**H**$_2$), 1.27 (5H, -C**H**$_2$C**H**(CH)$_3$C**H**$_2$CH$_3$), 1.09 (2H, -C**H**$_2$CH$_3$), 0.82 (6H, -CH(C**H**$_3$)CH$_2$C**H**$_3$)					

Table 8. ^{1}H-NMR (d_6-DMSO) characterization of D-Ala13, L-Ser12-relacidine B (**4b**)

Residue	-NH	Hα	Hβ	Hγ	Hδ	Hε
D-Ser1	7.88 (1H, d, *J* = 7.4 Hz)	4.27 (1H, m)	3.51 (2H, m)	5.14 (1H, br s)		
D-Tyr2	8.02 (1H, m)	4.35 (1H, m)	2.83 (1H, dd, *J* = 14.2, 4.3 Hz) & 2.62 (1H, m)	Phenol: 9.18 (1H, s), 6.90 (2H, d, *J* = 8.5 Hz), 6.57 (2H, d, *J* = 8.4 Hz)		
D-Trp3	8.01 (1H, m)	4.53 (1H, m)	3.16 (1H, dd, *J* = 15.0, 4.5 Hz) & 2.95 (1H, m)	Indole: 10.79 (1H, s), 7.58 (1H, d, *J* = 2.9 Hz), 7.34 (1H, d, *J* = 8.1 Hz), 7.15 (1H, d, *J* = 2.4 Hz), 7.07 (1H, t, *J* = 7.5 Hz), 6.99 (1H, t, *J* = 7.4 Hz)		
D-Orn4	8.03 (1H, m)	4.38 (1H, m)	1.73 (1H, m) & 1.56 (1H, m)	1.56 (2H, m)	2.78 (2H, m)	7.74 (2H, br m)
Orn5	8.09 (1H, d, *J* = 8.2 Hz)	4.41 (1H, m)	1.71 (1H, m) & 1.53 (1H, m)	1.53 (2H, m)	2.77 (2H, m)	7.74 (2H, br m)
Gly6	8.27 (1H, t, *J* = 5.6 Hz)	3.84 (1H, dd, *J* = 16.9, 6.0 Hz) & 3.72 (1H, dd, *J* = 16.8, 5.1 Hz)				
D-Orn7	8.11 (1H, d, *J* = 8.5 Hz)	4.38 (1H, m)	1.42 (1H, m) & 1.29 (1H, m)	1.35 (2H, m)	2.59 (2H, m)	7.66 (2H, br m)
Trp8	8.21 (1H, d, *J* = 8.1 Hz)	4,76 (1H, m)	3.13 (1H, dd, *J* = 14.6, 5.0 Hz) & 2.97 (1H, m)	Indole: 10.79 (1H, s), 7.57 (1H, d, *J* = 3.0 Hz), 7.31 (1H, d, *J* = 8.0 Hz), 7.10 (1H, d, *J* = 2.4 Hz), 7.04 (1H, t, *J* = 7.5 Hz), 6.95 (1H, t, *J* = 7.4 Hz)		
Thr9	7.95 (1H, d, *J* = 8.4 Hz)	4.58 (1H, dd, *J* = 8.4, 3.9 Hz)	5.07 (1H, m)	1.05 (3H, d, *J* = 6.5 Hz)		
Ile10	7.80 (1H, d, *J* = 9.4 Hz)	4.27 (1H, m)	1.74 (1H, m)	1.42 (1H, m) & 1.10 (1H, m), 0.84 (3H, m)	0.84 (3H, m)	
Gly11	8.96 (1H, t, *J* = 5.8 Hz)	3.95 (1H, dd, *J* = 14.0, 5.1 Hz) & 3.31 (1H, dd, *J* = 14.0, 6.4 Hz)				
Ser12	8.66 (1H, d, *J* = 7.8 Hz)	4.03 (1H, m)	3.65 (2H, m)	4.89 (1H, br s)		
D-Ala13	7.98 (1H, d, *J* = 7.5 Hz)	4.18 (1H, p, *J* = 7.1 Hz)	1.26 (3H, d, *J* = 7.0 Hz)			
Lipid	2.12 (2H, m, O=CC**H**$_2$), 1.50 (2H, O=CCH$_2$C**H**$_2$), 1.27 (5H, -C**H**$_2$C**H**(CH)$_3$C**H**$_2$CH$_3$), 1.09 (2H, -C**H**$_2$CH$_3$), 0.82 (6H, -CH(C**H**$_3$)CH$_2$C**H**$_3$)					

Table 9. ^{1}H-NMR (d_6-DMSO) characterization of L-Ala13, D-Ser12-relacidine B (**4c**)

Residue	-NH	Hα	Hβ	Hγ	Hδ	Hε
D-Ser1	7.88 (1H, d, *J* = 7.3 Hz)	4.26 (1H, q, *J* = 6.5 Hz)	3.52 (2H, m)	5.12 (1H, t, *J* = 5.5 Hz)		
D-Tyr2	8.02 (1H, m)	4.35 (1H, m)	2.83 (1H, dd, *J* = 14.2, 4.3 Hz) & 2.62 (1H, dd, *J* = 14.2, 9.5 Hz)	Phenol: 9.17 (1H, s), 6.89 (2H, m), 6.57 (2H, m)		
D-Trp3	8.00 (1H, m)	4.51 (1H, m)	3.16 (1H, m) & 2.95 (1H, dd, *J* = 15.0, 9.4 Hz)	Indole: 10.79 (1H, s), 7.57 (1H, d, *J* = 7.9 Hz), 7.34 (1H, d, *J* = 8.0 Hz), 7.15 (1H, m), 7.07 (1H, m), 6.99 (1H, m)		
D-Orn4	8.02 (1H, d, *J* = 8.4 Hz)	4.35 (1H, m)	1.73 (1H, m) & 1.56 (1H, m)	1.56 (2H, m)	2.77 (2H, m)	7.71 (2H, br m)
Orn5	8.08 (1H, d, *J* = 8.2 Hz)	4.41 (1H, m)	1.71 (1H, m) & 1.53 (1H, m)	1.53 (2H, m)	2.77 (2H, m)	7.71 (2H, br m)
Gly6	8.24 (1H, t, *J* = 5.6 Hz)	3.81 (1H, m) & 3.74 (1H, m)				
D-Orn7	8.04 (1H, d, *J* = 8.4 Hz)	4.38 (1H, m)	1.35 (1H, m) & 1.20 (1H, m)	1.25 (2H, m)	2.54 (2H, m)	7.61 (2H, br m)
Trp8	8.20 (1H, d, *J* = 8.2 Hz)	4,73 (1H, m)	3.16 (1H, m) & 2.90 (1H, dd, *J* = 14.7, 9.7 Hz)	Indole: 10.74 (1H, s), 7.66 (1H, d, *J* = 7.8 Hz), 7.31 (1H, d, *J* = 8.1 Hz), 7.15 (1H, m), 7.04 (1H, m), 6.96 (1H, m)		
Thr9	7.84 (1H, d, *J* = 8.9 Hz)	4.68 (1H, dd, *J* = 9.0, 2.8 Hz)	5.26 (1H, m)	1.13 (3H, d, *J* = 6.3 Hz)		
Ile10	8.39 (1H, d, *J* = 3.1 Hz)	3.82 (1H, m)	1.66 (1H, m)	1.61 (1H, m) & 1.20 (1H, m), 0.88 (3H, d, *J* = 6.7 Hz)	0.91 (3H, t, *J* = 7.3 Hz)	
Gly11	9.17 (1H, m)	3.75 (1H, m) & 3.62 (1H, m)				
D-Ser12	7.47 (1H, d, *J* = 9.0 Hz)	4.34 (1H, m)	3.99 (1H, m) & 3.84 (1H, m)	4.86 (1H, t, *J* = 6.6 Hz)		
Ala13	7.45 (1H, d, *J* = 9.2 Hz)	4.61 (1H, m)	1.18 (3H, d, *J* = 6.9 Hz)			
Lipid	2.12 (2H, m, O=CC**H**$_2$), 1.50 (2H, O=CCH$_2$C**H**$_2$), 1.27 (5H, -C**H**$_2$C**H**(CH)$_3$C**H**$_2$CH$_3$), 1.09 (2H, -C**H**$_2$CH$_3$), 0.82 (6H, -CH(C**H**$_3$)CH$_2$C**H**$_3$)					

Table 10. ^{1}H-NMR (d_6-DMSO) characterization of D-Ala13, D-Ser12-relacidine B (**4d**)

Residue	-NH	Hα	Hβ	Hγ	Hδ	Hε
D-Ser1	7.88 (1H, d, *J* = 7.4 Hz)	4.27 (1H, m)	3.51 (2H, m)	5.15 (1H, br s)		
D-Tyr2	8.02 (1H, m)	4.35 (1H, m)	2.83 (1H, dd, *J* = 14.2, 4.3 Hz) & 2.62 (1H, m)	Phenol: 9.18 (1H, s), 6.90 (2H, d, *J* = 8.5 Hz), 6.57 (2H, d, *J* = 8.3 Hz)		
D-Trp3	8.01 (1H, m)	4.52 (1H, m)	3.16 (1H, m) & 2.95 (1H, m)	Indole: 10.80 (1H, s), 7.58 (1H, t, *J* = 7.3 Hz), 7.34 (1H, d, *J* = 8.1 Hz), 7.15 (1H, d, *J* = 2.4 Hz), 7.07 (1H, t, *J* = 7.5 Hz), 6.99 (1H, t, *J* = 7.4 Hz)		
D-Orn4	8.03 (1H, m)	4.38 (1H, m)	1.73 (1H, m) & 1.56 (1H, m)	1.56 (2H, m)	2.78 (2H, m)	7.75 (2H, br m)
Orn5	8.09 (1H, m)	4.41 (1H, m)	1.71 (1H, m) & 1.53 (1H, m)	1.53 (2H, m)	2.77 (2H, m)	7.75 (2H, br m)
Gly6	8.25 (1H, t, *J* = 5.6 Hz)	3.83 (1H, dd, *J* = 17.0, 6.0 Hz) & 3.73 (1H, m)				
D-Orn7	8.11 (1H, m)	4.38 (1H, m)	1.41 (1H, m) & 1.29 (1H, m)	1.33 (2H, m)	2.59 (2H, m)	7.67 (2H, br m)
Trp8	8.20 (1H, d, *J* = 8.1 Hz)	4,78 (1H, m)	3.12 (1H, dd, *J* = 14.6, 4.9 Hz) & 2.96 (1H, m)	Indole: 10.78 (1H, s), 7.58 (1H, t, *J* = 7.3 Hz), 7.31 (1H, d, *J* = 8.0 Hz), 7.10 (1H, d, *J* = 2.4 Hz), 7.04 (1H, t, *J* = 7.5 Hz), 6.95 (1H, t, *J* = 7.4 Hz)		
Thr9	8.04 (1H, m)	4.65 (1H, dd, *J* = 8.4, 4.0 Hz)	5.05 (1H, m)	1.07 (3H, d, *J* = 6.4 Hz)		
Ile10	8.11 (1H, m)	4.24 (1H, t, *J* = 7.8 Hz)	1.68 (1H, m)	1.52 (1H, m) & 1.13 (1H, m), 0.86 (3H, m)	0.86 (3H, m)	
Gly11	8.97 (1H, t, *J* = 5.4 Hz)	3.73 (1H, m) & 3.58 (1H, m)				
D-Ser12	7.42 (1H, d, *J* = 9.0 Hz)	4.27 (1H, m)	3.71 (2H, m)	4.82 (1H, br s)		
D-Ala13	7.50 (1H, d, *J* = 6.9 Hz)	4.08 (1H, p, *J* = 7.1 Hz)	1.39 (3H, d, *J* = 7.1 Hz)			
Lipid	2.12 (2H, m, O=CC**H**$_2$), 1.50 (2H, O=CCH$_2$C**H**$_2$), 1.27 (5H, -C**H**$_2$C**H**(CH)$_3$C**H**$_2$CH$_3$), 1.09 (2H, -C**H**$_2$CH$_3$), 0.82 (6H, -CH(C**H**$_3$)CH$_2$C**H**$_3$)					

Table 11. ^{1}H-NMR (d_6-DMSO) characterization of relacidamide (**5**)

Residue	-NH	Hα	Hβ	Hγ	Hδ	Hε
D-Ser1	7.89 (1H, d, *J* = 7.4 Hz)	4.27 (1H, m)	3.51 (2H, m)	5.14 (1H, br s)		
D-Tyr2	8.02 (1H, m)	4.35 (1H, m)	2.83 (1H, dd, *J* = 14.3, 4.5 Hz) & 2.62 (1H, m)	Phenol: 9.18 (1H, s), 6.90 (2H, d, *J* = 8.5 Hz), 6.57 (2H, d, *J* = 8.4 Hz)		
D-Trp3	8.01 (1H, m)	4.52 (1H, m)	3.16 (1H, dd, *J* = 15.0, 4.5 Hz) & 2.95 (1H, dd, *J* = 14.9, 9.4 Hz)	Indole: 10.80 (1H, s), 7.60 (1H, d, *J* = 7.9 Hz), 7.34 (1H, d, *J* = 8.1 Hz), 7.15 (1H, d, *J* = 2.4 Hz), 7.07 (1H, t, *J* = 7.6 Hz), 6.99 (1H, t, *J* = 7.4 Hz)		
D-Orn4	8.03 (1H, m)	4.38 (1H, m)	1.74 (1H, m) & 1.57 (1H, m)	1.57 (2H, m)	2.78 (2H, m)	7.75 (2H, br m)
Orn5	8.09 (1H, d, *J* = 8.2 Hz)	4.41 (1H, m)	1.71 (1H, m) & 1.54 (1H, m)	1.54 (2H, m)	2.78 (2H, m)	7.75 (2H, br m)
Gly6	8.27 (1H, m)	3.80 (1H, dd, *J* = 16.8, 5.8 Hz) & 3.76 (1H, m)				
D-Orn7	8.07 (1H, d, *J* = 8.3 Hz)	4.33 (1H, m)	1.39 (1H, m) & 1.28 (1H, m)	1.32 (2H, m)	2.59 (2H, m)	7.66 (2H, br m)
Trp8	8.17 (1H, d, *J* = 8.3 Hz)	4,63 (1H, m)	3.10 (1H, m) & 2.90 (1H, dd, *J* = 14.7, 8.7 Hz)	Indole: 10.78 (1H, s), 7.58 (1H, d, *J* = 8.0 Hz), 7.31 (1H, d, *J* = 8.0 Hz), 7.10 (1H, d, *J* = 2.3 Hz), 7.04 (1H, t, *J* = 7.5 Hz), 6.97 (1H, t, *J* = 7.4 Hz)		
Dap9	8.22 (1H, d, *J* = 7.4 Hz)	4.27 (1H, m)	3.56 (1H, m) & 2.80 (1H, m)	6.83 (1H, t, *J* = 6.5 Hz)		
Ile10	8.27 (1H, m)	4.10 (1H, t, *J* = 9.7 Hz)	1.76 (1H, m)	1.56 (1H, m) & 1.16 (1H, m), 0.83 (3H, m)	0.84 (3H, t, *J* = 7.4 Hz)	
Gly11	9.02 (1H, t, *J* = 5.3 Hz)	3.95 (1H, dd, *J* = 14.8, 3.8 Hz) & 3.45 (1H, m)				
Ser12	9.00 (1H, d, *J* = 5.5 Hz)	3.91 (1H, m)	3.74 (1H, m) & 3.68 (1H, m)	5.07 (1H, br s)		
Gly13	7.95 (1H, m)	3.92 (1H, m) & 3.51 (1H, m)				
Lipid	2.12 (2H, m, O=CC**H**$_2$), 1.50 (2H, O=CCH$_2$C**H**$_2$), 1.27 (5H, -C**H**$_2$C**H**(CH)$_3$C**H**$_2$CH$_3$), 1.09 (2H, -C**H**$_2$CH$_3$), 0.82 (6H, -CH(C**H**$_3$)CH$_2$C**H**$_3$)					

NMR traces of all peptides can be found in the online supplementary material at DOI https://doi.org/10.1021/acsinfecdis.3c00043

Supplemental Figures

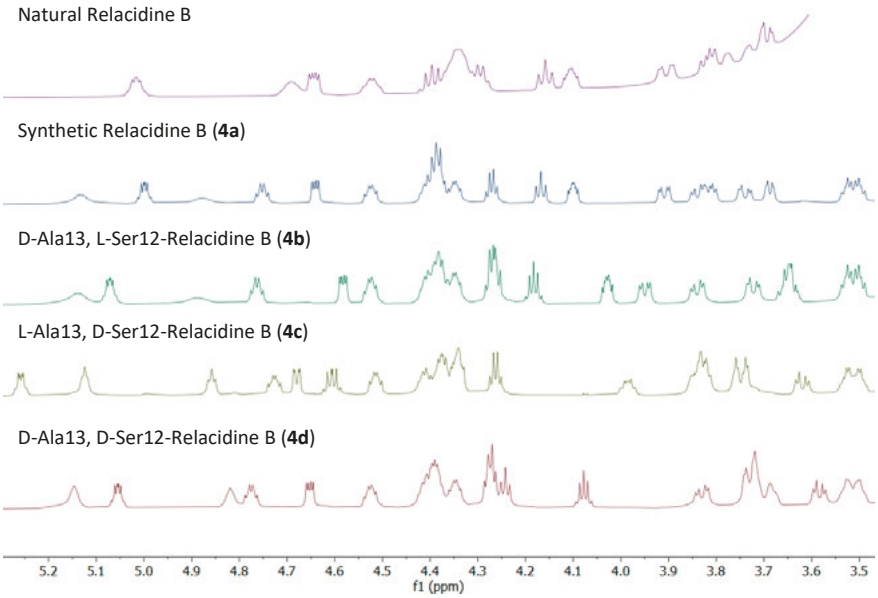

Figure S1. Previously published[9] ^{1}H-NMR (600 MHz, d_6-DMSO) spectrum of natural relacidine B isolated after fermentation of the producing organism overlaid with ^{1}H-NMR (850 MHz, d_6-DMSO) spectra of synthetic relacidines **4a**-**4d**. Spectra were recorded at room temperature.

References

(1) Murray, C. J.; Ikuta, K. S.; Sharara, F.; Swetschinski, L.; Robles Aguilar, G.; Gray, A.; Han, C.; Bisignano, C.; Rao, P.; Wool, E.; Johnson, S. C.; Browne, A. J.; Chipeta, M. G.; Fell, F.; Hackett, S.; Haines-Woodhouse, G.; Kashef Hamadani, B. H.; Kumaran, E. A. P.; McManigal, B.; Agarwal, R.; Akech, S.; Albertson, S.; Amuasi, J.; Andrews, J.; Aravkin, A.; Ashley, E.; Bailey, F.; Baker, S.; Basnyat, B.; Bekker, A.; Bender, R.; Bethou, A.; Bielicki, J.; Boonkasidecha, S.; Bukosia, J.; Carvalheiro, C.; Castañeda-Orjuela, C.; Chansamouth, V.; Chaurasia, S.; Chiurchiù, S.; Chowdhury, F.; Cook, A. J.; Cooper, B.; Cressey, T. R.; Criollo-Mora, E.; Cunningham, M.; Darboe, S.; Day, N. P. J.; De Luca, M.; Dokova, K.; Dramowski, A.; Dunachie, S. J.; Eckmanns, T.; Eibach, D.; Emami, A.; Feasey, N.; Fisher-Pearson, N.; Forrest, K.; Garrett, D.; Gastmeier, P.; Giref, A. Z.; Greer, R. C.; Gupta, V.; Haller, S.; Haselbeck, A.; Hay, S. I.; Holm, M.; Hopkins, S.; Iregbu, K. C.; Jacobs, J.; Jarovsky, D.; Javanmardi, F.; Khorana, M.; Kissoon, N.; Kobeissi, E.; Kostyanev, T.; Krapp, F.; Krumkamp, R.; Kumar, A.; Kyu, H. H.; Lim, C.; Limmathurotsakul, D.; Loftus, M. J.; Lunn, M.; Ma, J.; Mturi, N.; Munera-Huertas, T.; Musicha, P.; Mussi-Pinhata, M. M.; Nakamura, T.; Nanavati, R.; Nangia, S.; Newton, P.; Ngoun, C.; Novotney, A.; Nwakanma, D.; Obiero, C. W.; Olivas-Martinez, A.; Olliaro, P.; Ooko, E.; Ortiz-Brizuela, E.; Peleg, A. Y.; Perrone, C.; Plakkal, N.; Ponce-de-Leon, A.; Raad, M.; Ramdin, T.; Riddell, A.; Roberts, T.; Robotham, J. V.; Roca, A.; Rudd, K. E.; Russell, N.; Schnall, J.; Scott, J. A. G.; Shivamallappa, M.; Sifuentes-Osornio, J.; Steenkeste, N.; Stewardson, A. J.; Stoeva, T.; Tasak, N.; Thaiprakong, A.; Thwaites, G.; Turner, C.; Turner, P.; van Doorn, H. R.; Velaphi, S.; Vongpradith, A.; Vu, H.; Walsh, T.; Waner, S.; Wangrangsimakul, T.; Wozniak, T.; Zheng, P.; Sartorius, B.; Lopez, A. D.; Stergachis, A.; Moore, C.; Dolecek, C.; Naghavi, M. Global Burden of Bacterial Antimicrobial Resistance in 2019: A Systematic Analysis. *Lancet* **2022**, *399* (10325), 629–655. https://doi.org/10.1016/S0140-6736(21)02724-0.

(2) O'Neill, J. *Antimicrobial Resistance: Tackling a Crisis for the Health and Wealth of Nations.*; 2014.

(3) O'Neill, J. *Tackling Drug-Resistant Infections Globally: Final Report and Recommendations.*; London, 2016.

(4) CDC. *COVID-19: U.S. Impact on Antimicrobial Resistance, Special Report 2022*; Atlanta, Georgia, 2022. https://doi.org/10.15620/cdc:117915.

(5) Rice, L. B. Federal Funding for the Study of Antimicrobial Resistance in Nosocomial Pathogens: No ESKAPE. *Journal of Infectious Diseases*. Oxford Academic April 15, 2008, pp 1079–1081. https://doi.org/10.1086/533452.

(6) WHO. https://www.who.int/news-room/detail/27-02-2017-who-publishes-list-of-bacteria-for-which-new-antibiotics-are-urgently-needed.

(7) Li, Y. X.; Zhong, Z.; Zhang, W. P.; Qian, P. Y. Discovery of Cationic Nonribosomal Peptides as Gram-Negative Antibiotics through Global Genome Mining. *Nat. Commun.* **2018**, *9* (1). https://doi.org/10.1038/s41467-018-05781-6.

(8) Al Ayed, K.; Ballantine, R. D.; Hoekstra, M.; Bann, S. J.; Wesseling, C. M. J.; Bakker, A. T.; Zhong, Z.; Li, Y. X.; Brüchle, N. C.; van der Stelt, M.; Cochrane, S. A.; Martin, N. I. Synthetic Studies with the Brevicidine and Laterocidine Lipopeptide Antibiotics Including Analogues with Enhanced Properties and in Vivo Efficacy. *Chem. Sci.* **2022**, *13* (12), 3563–3570. https://doi.org/10.1039/d2sc00143h.

(9) Li, Z.; Chakraborty, P.; de Vries, R. H.; Song, C.; Zhao, X.; Roelfes, G.; Scheffers, D. J.; Kuipers, O. P. Characterization of Two Relacidines Belonging to a Novel Class of Circular Lipopeptides That Act against Gram-Negative Bacterial Pathogens. *Environ. Microbiol.* **2020**, *22* (12), 5125–5136. https://doi.org/10.1111/1462-2920.15145.

(10) Li, Z.; Song, C.; Yi, Y.; Kuipers, O. P. Characterization of Plant Growth-Promoting Rhizobacteria from Perennial Ryegrass and Genome Mining of Novel Antimicrobial Gene Clusters. *BMC Genomics* **2020**, *21* (1), 1–11. https://doi.org/10.1186/s12864-020-6563-7.

(11) Blin, K.; Shaw, S.; Kloosterman, A. M.; Charlop-Powers, Z.; van Wezel, G. P.; Medema, M. H.; Weber, T. AntiSMASH 6.0: Improving Cluster Detection and Comparison Capabilities. *Nucleic Acids Res.* **2021**, *49* (W1), W29–W35. https://doi.org/10.1093/nar/gkab335.

(12) Medema, M. H.; Kottmann, R.; Yilmaz, P.; Cummings, M.; Biggins, J. B.; Blin, K.; de Bruijn, I.; Chooi, Y. H.; Claesen, J.; Coates, R. C.; Cruz-Morales, P.; Duddela, S.; Düsterhus, S.; Edwards, D. J.; Fewer, D. P.; Garg, N.; Geiger, C.; Gomez-Escribano, J. P.; Greule, A.; Hadjithomas, M.; Haines, A. S.; Helfrich, E. J. N.; Hillwig, M. L.; Ishida, K.; Jones, A. C.; Jones, C. S.; Jungmann, K.; Kegler, C.; Kim, H. U.; Kötter, P.; Krug, D.; Masschelein, J.; Melnik, A. V.; Mantovani, S. M.; Monroe, E. A.; Moore, M.; Moss, N.; Nützmann, H.-W.; Pan, G.; Pati, A.; Petras, D.; Reen, F. J.; Rosconi, F.; Rui, Z.; Tian, Z.; Tobias, N. J.; Tsunematsu, Y.; Wiemann, P.; Wyckoff, E.; Yan, X.; Yim, G.; Yu, F.; Xie, Y.; Aigle, B.; Apel, A. K.; Balibar, C. J.; Balskus, E. P.; Barona-Gómez, F.; Bechthold, A.; Bode, H. B.; Borriss, R.; Brady, S. F.; Brakhage, A. A.; Caffrey, P.; Cheng, Y.-Q.; Clardy, J.; Cox, R. J.; De Mot, R.; Donadio, S.; Donia, M. S.; van der Donk, W. A.; Dorrestein, P. C.; Doyle, S.; Driessen, A. J. M.; Ehling-Schulz, M.; Entian, K.-D.; Fischbach, M. A.; Gerwick, L.; Gerwick, W. H.; Gross, H.; Gust, B.; Hertweck, C.; Höfte, M.; Jensen, S. E.; Ju, J.; Katz, L.; Kaysser, L.; Klassen, J. L.; Keller, N. P.; Kormanec, J.; Kuipers, O. P.; Kuzuyama, T.; Kyrpides, N. C.; Kwon, H.-J.; Lautru, S.; Lavigne, R.; Lee, C. Y.; Linquan, B.; Liu, X.; Liu, W.; Luzhetskyy, A.; Mahmud, T.; Mast, Y.; Méndez, C.; Metsä-Ketelä, M.; Micklefield, J.; Mitchell, D. A.; Moore, B. S.; Moreira, L. M.; Müller, R.; Neilan, B. A.; Nett, M.; Nielsen, J.; O'Gara, F.; Oikawa, H.; Osbourn, A.; Osburne, M. S.; Ostash, B.; Payne, S. M.; Pernodet, J.-L.; Petricek, M.; Piel, J.; Ploux, O.; Raaijmakers, J. M.; Salas, J. A.; Schmitt, E. K.; Scott, B.; Seipke, R. F.; Shen, B.; Sherman, D. H.; Sivonen, K.; Smanski, M. J.; Sosio, M.; Stegmann, E.; Süssmuth, R. D.; Tahlan, K.; Thomas, C. M.; Tang, Y.; Truman, A. W.; Viaud, M.; Walton, J. D.; Walsh, C. T.; Weber, T.; van Wezel, G. P.; Wilkinson, B.; Willey, J. M.; Wohlleben, W.; Wright, G. D.; Ziemert, N.; Zhang, C.; Zotchev, S. B.; Breitling, R.; Takano, E.; Glöckner, F. O. Minimum Information about a Biosynthetic Gene Cluster. *Nat. Chem. Biol.* **2015**, *11* (9), 625–631. https://doi.org/10.1038/nchembio.1890.

(13) Jumper, J.; Evans, R.; Pritzel, A.; Green, T.; Figurnov, M.; Ronneberger, O.; Tunyasuvunakool, K.; Bates, R.; Žídek, A.; Potapenko, A.; Bridgland, A.; Meyer, C.; Kohl, S. A. A.; Ballard, A. J.; Cowie, A.; Romera-Paredes, B.; Nikolov, S.; Jain, R.; Adler, J.; Back, T.; Petersen, S.; Reiman, D.; Clancy, E.; Zielinski, M.; Steinegger, M.; Pacholska, M.; Berghammer, T.; Bodenstein, S.; Silver, D.; Vinyals, O.; Senior, A. W.; Kavukcuoglu, K.; Kohli, P.; Hassabis, D. Highly Accurate Protein Structure Prediction with AlphaFold. *Nature* **2021**, *596* (7873), 583–589. https://doi.org/10.1038/s41586-021-03819-2.

(14) Ballantine, R. D.; Al Ayed, K.; Bann, S. J.; Hoekstra, M.; Martin, N. I.; Cochrane, S. A. Synthesis and Structure–

Activity Relationship Studies of N-Terminal Analogues of the Lipopeptide Antibiotics Brevicidine and Laterocidine. *RSC Med. Chem.* **2022**, *00*, 1–3. https://doi.org/10.1039/d2md00281g.

(15) Tsai, C. J.-Y.; Loh, J. M. S.; Proft, T. Galleria Mellonella Infection Models for the Study of Bacterial Diseases and for Antimicrobial Drug Testing. *Virulence* **2016**, *7* (3), 214–229. https://doi.org/10.1080/21505594.2015.1135289.

(16) Pereira, M. F.; Rossi, C. C.; da Silva, G. C.; Rosa, J. N.; Bazzolli, D. M. S. Galleria Mellonella as an Infection Model: An in-Depth Look at Why It Works and Practical Considerations for Successful Application. *Pathog. Dis.* **2020**, *78* (8), 56. https://doi.org/10.1093/femspd/ftaa056.

(17) Mukherjee, S.; Van Der Donk, W. A. Mechanistic Studies on the Substrate-Tolerant Lanthipeptide Synthetase ProcM. *J. Am. Chem. Soc.* **2014**, *136* (29), 10450–10459. https://doi.org/10.1021/ja504692v.

(18) Dexter, H. L.; Williams, H. E. L.; Lewis, W.; Moody, C. J. Total Synthesis of the Post-Translationally Modified Polyazole Peptide Antibiotic Goadsporin. *Angew. Chemie Int. Ed.* **2017**, *56* (11), 3069–3073. https://doi.org/10.1002/ANIE.201612103.

(19) Xiao, X.; Elsayed, S. S.; Wu, C.; Van Der Heul, H. U.; Metsä-Ketelä, M.; Du, C.; Prota, A. E.; Chen, C. C.; Liu, W.; Guo, R. T.; Abrahams, J. P.; Van Wezel, G. P. Functional and Structural Insights into a Novel Promiscuous Ketoreductase of the Lugdunomycin Biosynthetic Pathway. *ACS Chem. Biol.* **2020**, *15* (9), 2529–2538. https://doi.org/10.1021/acschembio.0c00564.

(20) Trebosc, V.; Gartenmann, S.; Tötzl, M.; Lucchini, V.; Schellhorn, B.; Pieren, M.; Lociuro, S.; Gitzinger, M.; Tigges, M.; Bumann, D.; Kemmer, C. Dissecting Colistin Resistance Mechanisms in Extensively Drug-Resistant Acinetobacter Baumannii Clinical Isolates. *MBio* **2019**, *10* (4). https://doi.org/10.1128/mBio.01083-19.